ANALYSING CYLINDRICAL CAVITY LOADING TESTS USING HIGH RESOLUTION PRESSUREMETERS

SHEAR MODULUS & INSITU LATERAL STRESS

Cambridge Insitu Ltd
Little Eversden,
Cambridge,
CB23 1HE
ENGLAND

Email : cam@cambridge-insitu.com
www.cambridge-insitu.com
Tel : +44 (0)1223 262361

Table of Contents

PREFACE

This document is a partial description of the methods and procedures used by Cambridge Insitu Ltd (CI) to interpret cavity loading tests carried out using equipment manufactured by CI. These devices read pressure changes to better than 0.5kPa and radial displacement changes to better than 0.5 micrometres (5×10^{-7} metres). For a typical cavity this is a strain of 10^{-5}.

Some parts of this document may be applicable to third-party devices but do not assume this is the case.

The text covers all the analyses provided by the WINSITU software program and some further procedures that are not yet fully implemented. It uses examples from a wide range of sources to illustrate the arguments presented.

- Part 1 is an introduction and includes a description of how strains are calculated
- Part 2 concentrates on modulus
- Part 3 considers how to identify the Insitu lateral stress

ANALYSING CYLINDRICAL CAVITY LOADING TESTS

PART 1 - INTRODUCTION

1 MATERIAL PROPERTIES FROM PRESSUREMETER TESTS IN SOIL

1.1 Notation

ρ a small radial displacement

r any radius

r_c radius of cavity

r_o initial radius of cavity

p_c total pressure applied to cavity wall

p_o cavity reference pressure

P_f total yield stress

ε_r radial strain

ε_θ circumferential (hoop) strain

ε_c circumferential (hoop) strain at the cavity wall

c_u undrained shear strength

G shear modulus

σ_r radial stress

σ_θ circumferential stress

1.2 Introduction

A pressuremeter is one of a small number of tools capable of deriving representative parameters for critical engineering properties of dilatant or granular materials. It is unique in being able to provide strength and stiffness in a single test episode. The difficulty of the test is that these parameters are not directly measured but are discovered by solving the boundary value problem.

1.3 Ménard Pressuremeter

It is possible to avoid this restriction, at the cost of sacrificing the wider benefits of fundamental analysis. The Ménard system uses an approach that converts field data to a small number of quasi-parameters specific to the equipment and test procedures. Using correlations that have been obtained by relating pressuremeter data to the response of finished structures these parameters are inserted directly into semi-empirical design equations.

Avoiding fundamental analysis reduces the significance of the individual test. Essentially a Menard result is a superior version of a blow-count obtained from a Standard Penetration Test (SPT). Like the SPT, multiple tests at fairly closely-spaced levels are required in order to quantify the uncertainty.

Because of the method specificity there is no incentive to innovate the probe. It remains much as it did at its inception in 1957, a passive measuring device that makes comparatively coarse determinations of volume change.

The Ménard approach will not be considered any further here although it is as well to be aware that the overwhelming majority of pressuremeter tests carried out still use equipment and methods based on Ménard practice.

1.4 Disturbance

The aim of the pressuremeter test is to expand a long cylindrical cavity within an undisturbed mass of soil. Readings are taken of the pressure applied to the cavity wall and the consequent displacement. A modern pressuremeter test is a set of hundreds of co-ordinates that define a loading and unloading curve.

In practice no instrument can be placed into the ground without affecting the surrounding soil. In the case of a self-bored pressuremeter test the disturbance is less than that required to make the material yield (less than 1% shear strain) and is straightforward to allow for in the analysis procedure. This is an unusual situation in the context of soil investigation and most pressuremeter testing involves more disruptive means of getting an instrument into the ground that cause the material to fail either in extension or contraction. Once the material fails, the consequences for the test are irreversible. If the zone of disturbed material remains thin in relation to the expansion capability of the system, as is often the case for pre-bored testing, it may be possible eventually to see loading data that is a function of the true stress/strain properties of the material . If the material has been pushed then no amount of expansion will ever achieve this state – the best that can be achieved is reaching a limiting stress condition for an indeterminate strain. This is the case for devices such as a Cone Penetrometer (CPT), SPT and Cone Pressuremeter (CPM).

Irrecoverable disturbance is not the same thing as saying sensible parameters cannot be obtained from the test. Regardless of how the hole has been formed, it is always possible to expand the zone of disturbed material even further and in the process of doing so put every element of soil in that zone into a uniform plastic state. The insertion effects are then over-written and importantly, at single boundary remote from the cavity wall the material will be on the point of yielding. If the direction of loading is now reversed and the cavity forced to contract, then all the co-ordinates of pressure and displacement seen at the cavity wall will be a function of the remote boundary unloading elastically and eventually plastically if the contraction is continued. Assuming that the resolution of the measuring system is sufficient to see elastic movement, then using this technique means that a pushed test and a self-bored test are capable of providing similar quality results for stiffness and strength.

The primary reason for using self-boring instead of more invasive techniques is that to a large extent the initial stress state is preserved and the possibility of directly determining the horizontal geostatic stress σ_{ho} becomes available. This is harder to accomplish with more disruptive insertion methods. Invasive techniques are also more dependent on the applied solution being appropriate. The self boring test is able to assess the uncertainty of that assumption.

1.5 The pressuremeter test in soil - initially elastic response/failure in shear.

Solving the cylindrical cavity boundary problem means identifying the radial and

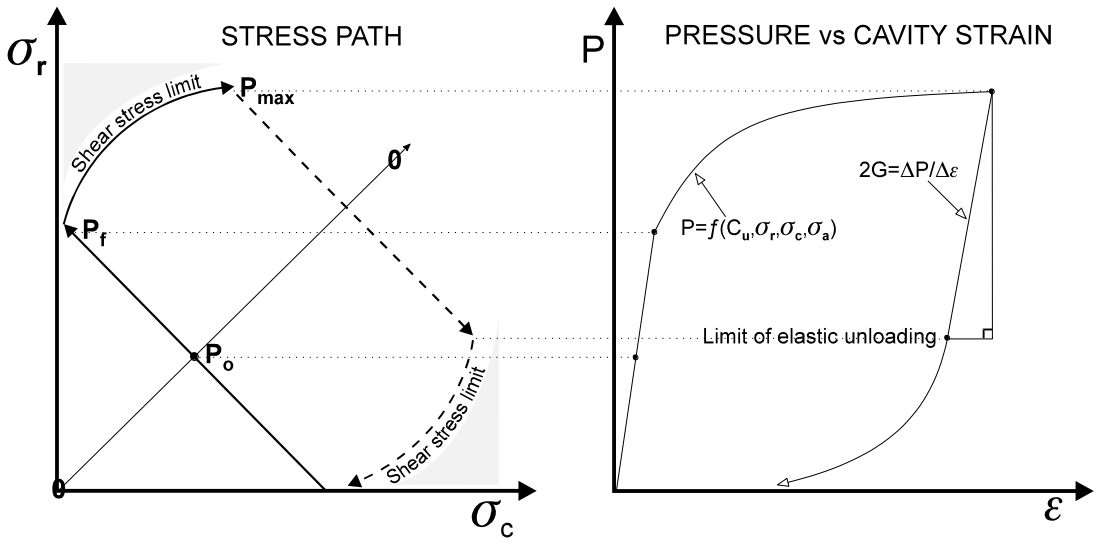

Figure 1.1 Elastic Response followed by failure in shear

circumferential strains ε_r and ε_θ, and the radial and circumferential effective stresses σ_r and σ_θ. Given any three, the fourth can be calculated. If the four parameters are known for one boundary, then they are calculable for all. For the boundary that is the cavity wall, ε_θ and σ_r are obtained directly from measurements the pressuremeter provides of radial displacement and total pressure.

Consider that the soil is homogeneous, and shows simple elastic behaviour before failing in shear. The stress path followed by an element of soil adjacent to the cavity is given in Figure 1.1 and the corresponding pressure/strain curve is shown alongside.

The radial stress, ideally at the insitu horizontal stress for a perfect installation, increases at the same rate as the circumferential stress decreases, regardless of whether the material is deforming under plane strain or plane stress conditions. The line 0 - 0 represents stress equality, so that in the ideal case considered here the point P_0 is the insitu lateral stress σ_{ho}.

Once the radial stress increases above P_0 then the shear stress in the soil at the cavity wall will increase. If P_0 is low, then it is possible that the circumferential stress would go into tension. The characteristic of soils is that the insitu stress is high enough to ensure that the shear stress limit is reached before tensile stresses can be generated. Tensile failure, as may be seen in rock, therefore implies comparatively low values for the initial stress state compared to the shear strength.

The pressure necessary to initiate shear failure is denoted p_f in fig 1. After this pressure the current slope of the field curve reduces steadily. The form of this part of the pressure/strain curve is a function of the shear strength of the material.

After the initial shear failure, radial stress and circumferential stress increase together. If the shear stress limit is constant, and is not influenced by pressure, and if the material deforms at constant volume then the failure shear strength can be determined by the analytical solution developed by Gibson & Anderson (1961). If the shear stress limit

increases as the loading develops then the solution of Hughes et al (1977) could be applied to discover the internal angle of friction and dilation.

Prior to reaching the shear stress limit, the pressuremeter response is elastic, both in loading and unloading. Assuming the soil deforms at a constant modulus and the installation is perfect then the slope of the initial loading path gives the shear modulus of the material, using the classic procedure of Bishop, Hill & Mott (1945). The diagram also indicates that reversing the direction of loading causes an initial elastic response giving an alternative means of deriving the shear modulus. This implies that small cycles of unloading and reloading taken anywhere in a test after reaching the shear stress limit can be used as a source of stiffness information (Hughes 1982).

As fig 1.1 indicates, the complete unloading of the pressuremeter can also be used to give strength and stiffness parameters comparable with those obtained from the loading path.

From the right hand side of the stress diagram it is apparent that the pressuremeter provides only a limited set of the necessary information for resolving the stresses and strains around the probe. Specifically it gives the changes in radius of the borehole wall (a special case of hoop strain) and the corresponding changes in radial stress at the borehole wall. There are no data for hoop stress or radial strain or movements in the vertical direction. Test procedures are chosen to allow the missing data to be inferred – for example an undrained expansion means shearing occurs at constant volume and hence changes of radial strain must be equal and opposite to changes in hoop strain. The unseen vertical axis data are rendered insignificant by making pressuremeters long with respect to their diameter, allowing plane strain expansion to be assumed.

1.6 Strain definitions

Fig 1.2 Stresses and strain around expanding cavity

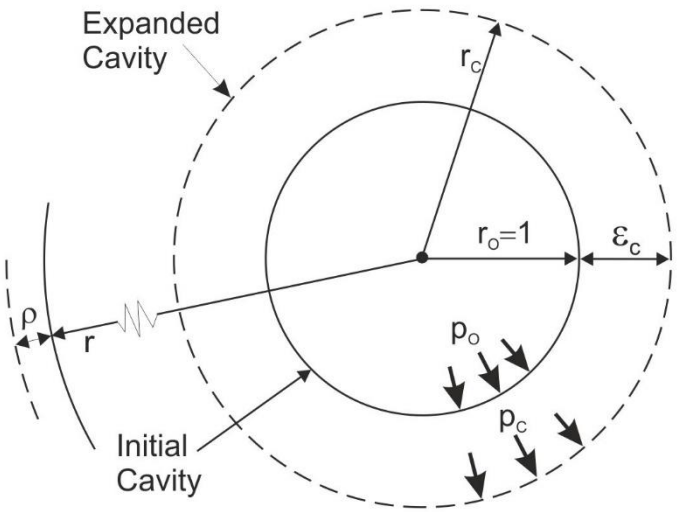

TERMS

ρ is a small radial displacement

r is any radius

r_c is radius of cavity

r_o is initial radius of cavity

p_c is pressure applied to cavity wall

p_o is cavity reference pressure

ε_c is circumferential (hoop) strain at the cavity wall

1.6.1 Simple strain

For a pressuremeter measuring the radius of an expanding cavity the conversion from displacement to simple strain is :

$$\varepsilon = [r_c - r_0]/r_0 \quad [1.1]$$

where r_c is the current radius of the cavity

r_0 is the original radius of the cavity *in the insitu state*.

ε is normally written ε_c to denote cavity strain. This is a particular case of circumferential or hoop strain. ε_c is often expressed as a percentage and by convention increases in the positive direction as the cavity enlarges. The physical reality is that hoop strain reduces as the cavity radius increases.

For a self bored cavity r_0 can be approximated by the at-rest radius of the instrument. This is unlikely to be the case for a stress relieved pocket. In general the approach then is to identify when the applied pressure has reached the insitu lateral stress, and interpolate from this the corresponding radius, which becomes r_0. As the analysis process goes through stages of iteration r_0 is likely to be re-defined again.

1.6.2 Current cavity strain

Current cavity strain is given by:

$$[r_c - r_0]/r_c \quad [1.2]$$

using the same terminology as above. This takes some account of alterations to the length of the displacement reference.

1.6.3 True or natural strain

If strains are small enough then the variation in the length of the displacement reference is insignificant. This is not the case for a pushed pressuremeter test which will result in the material experiencing very large strains. It is necessary then to use true or natural strain to describe the cavity deformation. This is the sum of the incremental increase in radius divided by the current radius:

$$\varepsilon = Ln[r_c/r_0] = Ln[1 + \varepsilon_c]. \quad [1.3]$$

Note –

When carrying out unload/reload cycles the calculation for shear modulus G is approximately

$$2G = \left[\frac{\Delta p_c}{\Delta \varepsilon_c}\right] \quad [1.4]$$

As pointed out by Mair & Wood (1987) this approximation is only justified for strains derived close to the origin and [1.4] should take account of the changing cavity radius:

$$2G = \left[\frac{r_c}{r_o}\right]\left[\frac{\Delta p_c}{\Delta \varepsilon_c}\right] \quad [1.5]$$

If true strain is used to calculate $d\epsilon_c$ then the additional term is not required and [1.4] is correct.

1.6.4 Shear strain

For material that is deforming at constant volume then the shear strain at the cavity wall γ_c is given by the constant area ratio, ΔA/A, which is the change of area divided by the current area. Referring to fig 1.2 where the cavity starts from unit radius:

$$\frac{\Delta A}{A} = \frac{\pi(1+\varepsilon_c)^2 - \pi}{\pi(1+\varepsilon_c)^2} \qquad [1.6]$$

$$\therefore \gamma_c = 1\text{-}1/(1+\varepsilon_c)^2$$

Note that γ_c can be expressed in terms of simple strain. Note also that when ε_c is less than 0.01 (1%) then $\gamma_c \approx 2\varepsilon_c$. The error is less than 2%.

For material that is not deforming at constant volume, calculating shear strain is more complex and depends on additional calculations that provide the increments of volumetric strain. These are explained in the section on analysing tests in drained materials.

1.7 Average displacements versus the output of the separate axes

There are a number of displacement sensors in the expansion probe but recommended practice is to quote parameters from the average displacement curve. This is for two reasons:

- The reference for the measured displacements is the body of the instrument itself - trying to separate the individual axes means assuming the body of the instrument remains fixed at all times, which is not realistic.
- All available analyses assume isotropic properties in the surrounding soil, and only the average pressure/strain curve represents this condition.

These remarks assume that the instrument is in full working order throughout the test - failure of a displacement follower means that alternative strategies must be adopted.

The significance of the first point above has been demonstrated by an examination of cycles of unloading taken from separate arms (Whittle 1993) and by work with a six arm version of the SBP (Whittle et al 1995). In the case of the 3 arm SBP an exception is sometimes made for the initial part of the loading prior to yield. In such circumstances the response of the separate arms may yield clues to the initial stress state in the surrounding soil, allowing an assessment of the degree of insertion disturbance.

1.8 The analysis program

We use (and supply to others) software for analysing a pressuremeter test. The program is called **WINSITU,** it has been in use for a number of years.

To use the program the user must first read in a text file of test data in engineering units. The program needs to know the type of instrument being used, and the user may choose to enter additional background information about the test.

The next task is to identify for the program the nature of the individual data points. Generally, the options are these:

- a point can be part of the expansion curve
- or part of a reload loop

- or part of the contraction curve
- or none of the above, and should be ignored in any analysis. This might mean a 'rogue' data point, but it is more likely to be true of parts of the loading where the expansion was slowed prior to taking an unload/reload cycle. Data points recorded at this time are neither part of the expansion nor part of a cycle.

There is a quick on-screen routine for marking the points. Once marked, they appear in different colours. Most of the analyses use a limited set of the available data - for example the Gibson & Anderson analysis for undrained shear strength uses only points on the expansion curve.

The program implements a number of standard analyses mainly in a graphical form. As fig 1.1 implies, there are significant changes of gradient in the pressure/strain curve denoting critical soil parameters. The user of the program is provided with on-screen tools to mark these breakpoints or to obtain the slope of the loading curve. The tools can be visualised as rulers, whose position is stored by the program in the file of test data. The evidence for any derived parameter is a screen drop of the relevant analysis that shows the position of any rulers set by the user and quotes the parameter obtained.

Even when the user declines to make a choice it may be good practice to provide the screen dump as evidence of why a choice is difficult.

The results for a test appear as a summary sheet of derived parameters followed by plots showing the application of the various procedures.

Sometimes analyses are required which are not included in the WINSITU program. In such instances commonly available spreadsheet software is used to implement the new analysis. Inevitably in such circumstances there is some risk of human error affecting the conversion of data in engineering units to the form required for analysis. WINSITU has export facilities and wherever possible is used as the data source for the spreadsheet.

ANALYSING CYLINDRICAL CAVITY LOADING TESTS

PART 2 DETERMINING MODULUS

2 DETERMINING MODULUS

2.1 Notation:

c_u	Undrained shear strength
G_i	Initial shear modulus
G_S	Secant shear modulus
G_t	Tangential shear modulus
G_y	Secant shear modulus when the material first reaches full plasticity (yield)
G_{max}	Elastic shear modulus
G_{hh}, G_{vh}	Shear moduli for transversely isotropic material
E_h, E_v	Young's modulus in the horizontal and vertical direction
ν	Poisson's ratio
ν_{hh}, ν_{hv}	Poisson's ratios for transversely isotropic material
m	Exponent of curvature used in modified hyperbolic equation
N	Exponent (Whittle & Liu, 2013)
n	Stress level exponent (Janbu, 1963) or anisotropy ratio (Wroth et al, 1979)
k_O	Ratio of horizontal to vertical effective insitu stress
τ, τ_c	Shear stress, suffix c means at the cavity wall
p_C	Pressure measured at the cavity wall
p'_o	Initial effective cavity reference stress
ε_c	Circumferential strain measured at the borehole wall
γ	Shear strain
γ_c	Shear strain measured at the borehole wall
γ_a	Invariant shear strain (axial strain in a triaxial test)
γ_{ref}	Reference shear strain when G_s will be $G_{max}/2$
γ_y	Shear strain at which the material reaches first failure
η	Radial stress constant when the strain scale is shear strain
η_h	Radial stress constant when the strain scale is cavity strain
α	Shear stress constant when the strain scale is shear strain
α_{ref}	Shear stress constant at a reference stress level
β	Exponent of non-linearity
σ'_{av}	Mean effective stress
σ_{ho} σ'_{ho}	Total and effective insitu lateral stress
σ_{vo} σ'_{vo}	Total and effective insitu vertical stress

2.2 Background

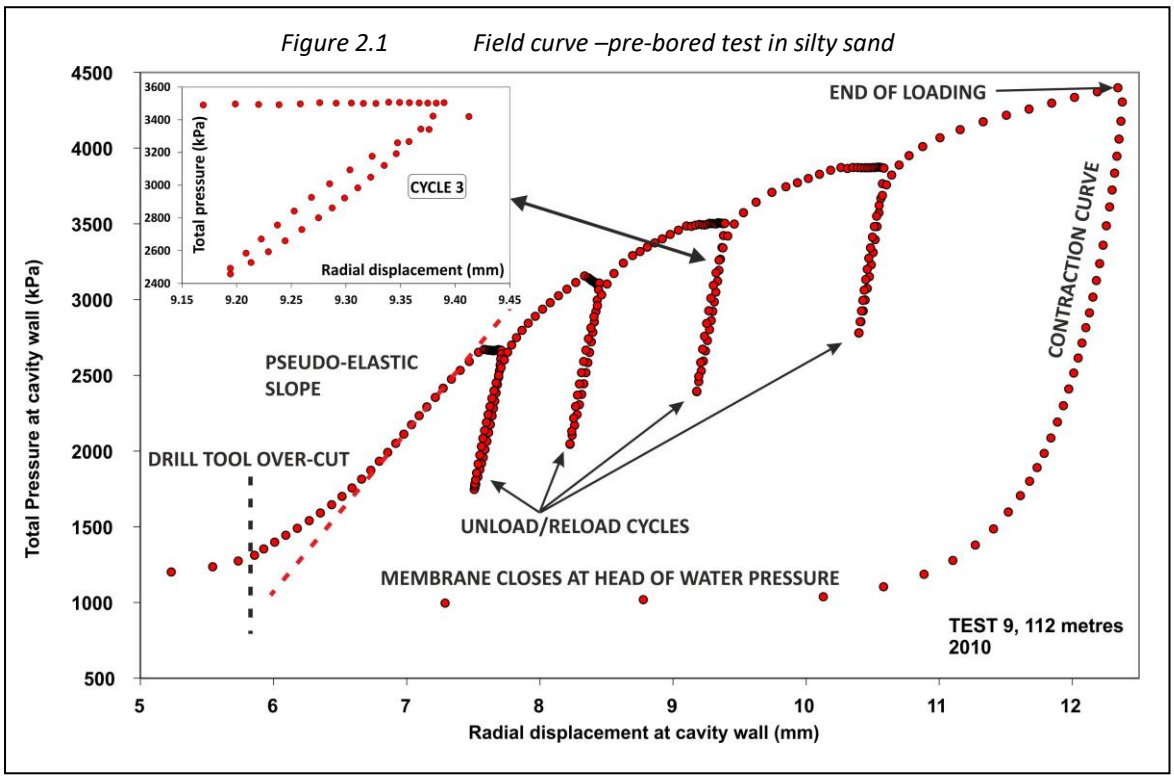

Figure 2.1 Field curve –pre-bored test in silty sand

For users of high resolution pressuremeter data the primary purpose of the test is obtaining realistic parameters for the elastic properties of the ground. Up to yield, where yield is defined as the first instance of mobilising the maximum shear stress, the slope of the loading curve can be used as a source of stiffness data. In practice this part of the cavity loading will be affected by disturbance, difficult to quantify, caused by the method used to place the probe in the ground (fig 1, the pseudo-elastic slope).

Once the material is loaded past its yield condition a zone of plastically deformed material starting from the cavity wall begins to extend into the soil mass. One consequence is that the stress history of the insertion process is erased as all elements within the plastic zone are put into a uniform condition. At a radius remote from the cavity wall and the pressuremeter there will be a single boundary where the material is on the point of yielding. If the direction of loading is reversed, the response seen at the pressuremeter will be that of the material beyond the boundary being unloaded elastically and then plastically. If the unloading continues then reverse plastic yield will result.

In fig 2.1, small cycles of unloading and reloading exploit the response prior to the reverse yield condition to derive the elastic properties of the ground. It is evident that although each cycle is taken at a different cavity radius and stress, the procedure is highly repeatable. This test was pre-bored, so the cavity was completely unloaded prior to the pressuremeter test commencing. The consequences of this are clear when the slope of the initial loading is compared to the unload/reload cycles.

It would be straightforward to place a line through each of the cycles in fig 2.1 and use the slope to calculate the shear modulus, G. This is common practice but, unless the material is intact rock, is misleading. The third cycle in fig 2.1 is shown as an inset, and has a clear hysteretic characteristic. This is due primarily to the influence of strain level on the current

modulus. The elastic response of the ground where all deformation is fully recoverable applies to a strain level beyond the reliable resolution of the pressuremeter at shear strains of about 0.002%. The unload/reload cycles are showing the largely recoverable response when the stress alteration is less than that required to make the material yield, shear strains in the range 0.01% to 1%. This is the strain range that is significant for design purposes.

If there are sufficient data in the cycle then it is possible take tangents to the unload or reload path of radial stress against cavity strain and find the current shear stress (Palmer 1972), as in fig 2.6. It is straightforward to turn these shear stress values into a shear modulus degradation trend. In practice the quantity of data are limited and the alternative is finding a function that describes the unload or reload path. Bolton & Whittle (1999) shows that this non-linear response is adequately represented by a power law. Using the power law parameters to solve the Palmer semi-differential solution gives a continuous stiffness degradation curve (figs 2.2 and 2.3). The individual points in these figures are the product of taking tangents to the measured data, the lines are the power law trend. Alternatives to the power law method include Jardine (1992) where a 'transformed strain' approach is applied to unload/reload data. The semi-empirical formulations were developed for specific soil types and are not transferable.

Figure 2.2 *Shear modulus degradation curves (drained loading)*

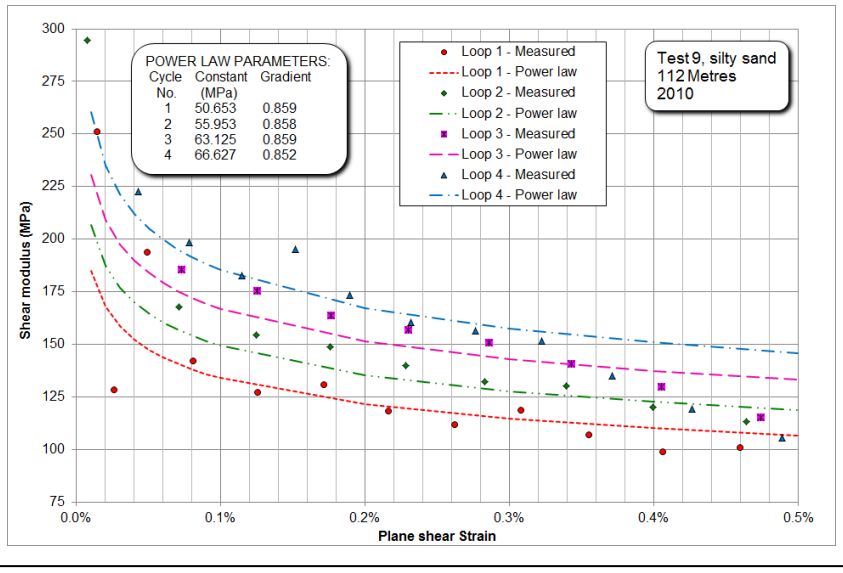

Figure 2.3 *Shear modulus degradation curves (undrained loading)*

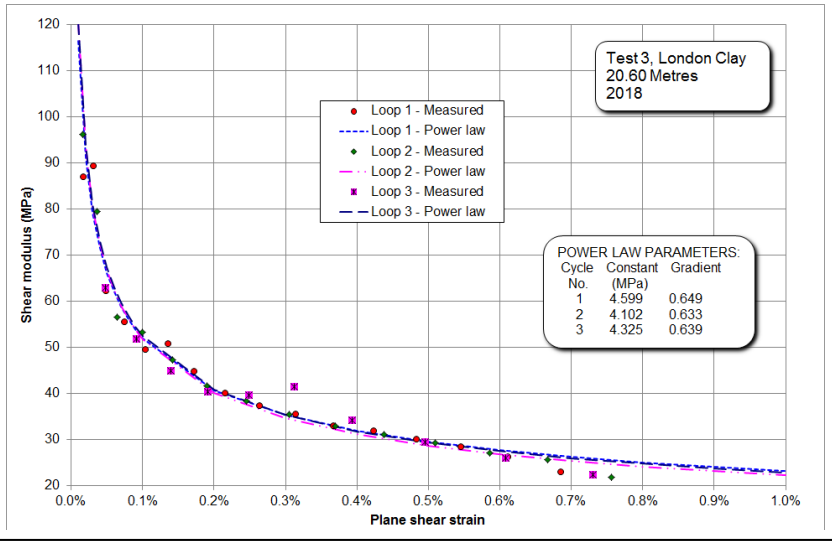

If the material is low permeability clay, giving an undrained loading, then the mean effective stress σ'_{av} following yield is constant, and all cycles will follow a similar path (fig 2.3).

The material tested in fig 2.1 is a silty sand and the loading is a drained event. The trend of each cycle (the strain dependency) is almost identical, but successive cycles (fig 2.2) plot a higher stiffness, because of increasing mean effective stress, σ'_{av}. A full data reduction will adjust these trends to a reference stress level such as the effective insitu lateral stress, σ'_{ho}. This requires σ'_{av} for each

cycle to be calculated. Hence although stiffness is obtainable from all insertion methods, no matter how disturbed, it may still be necessary to determine additional strength related parameters in order fully to reconcile the stiffness data.

Used vertically, the pressuremeter gives shear modulus parameters of type G_{hh}, where the first suffix shows the direction of loading and the second the direction of particle movement. Many design calculations requiring a value for shear modulus mean in practice the independent shear modulus G_{vh}. It is not possible to discover the ratio connecting G_{hh} and G_{vh} from a conventional pressuremeter test unless it is assumed that the ratio is related to k_o. This is only partly true. Nevertheless, because of the quality and relative speed with which G_{hh} can be determined it may be convenient to measure G_{hh} and assume an appropriate reduction factor. For engineering problems where the direction of loading is lateral, G_{hh} is the most relevant stiffness parameter.

Unloading and reloading are a feature of many laboratory material test procedures and pile loading tests. In the context of a cavity expansion in an infinite medium the first account of the theory behind the procedure is given by Hughes'82. Cycles are a prominent feature of the Wroth Rankine lecture (Wroth, '84). Bellotti et al ('89) give an explanation and methodology for manipulating the stress dependency of tests in sand. Muir Wood (1990) and Jardine (1992) explore the potential of the cycles for describing the non-linear strain dependency of the ground. Bolton & Whittle ('99) propose the simple procedure (described below) based on a power function.

Examining the detail within an unload/reload event requires high resolution local displacement measurement. Even in devices that do use local measurement it is necessary to be certain that what is measured is an accurate representation of the movements of the cavity wall, and not the finite stiffness of the probe itself.

The pressuremeter test shears the material. The modulus measured is shear modulus G and is independent of Poisson's ratio ν. G can be used to derive Young's modulus E but ν must be given or estimated. It is also straightforward to derive the bulk modulus M from the shear modulus.

Fig 2.4 Annotated unload/reload cycle

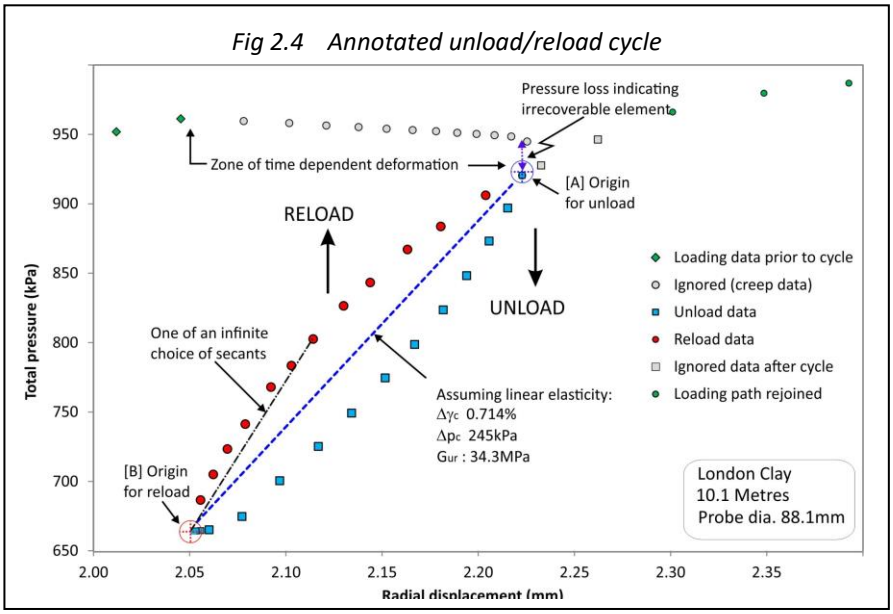

2.3 Describing the unload/reload cycle

Figure 2.4 shows an unload/reload cycle extracted from a field curve such as the example in fig 2.1. In this case the data are part of a test in stiff clay. In the interval between pausing the loading to take the cycle and the actual reversal of stress there are several data points showing the expansion continuing for no pressure increase.

This phase of time dependent deformation is referred to as 'creep'. Separating the contribution of the multiple processes that contribute to this behaviour is complex. It is unlikely that it will be possible to wait long enough for all creep behaviour to cease. This test in clay is an undrained event. There is a large excess pore pressure in the soil mass at the commencement of the cycle and waiting more than a short time would allow consolidation to take place. However the reducing displacement between readings shows that creep has fallen to a level low enough to permit a cycle to be taken.

The decrease of pressure continues until sufficient data has been recorded to give a clear indication of the path of the unloading response. The pressure decrease needs to be less than that required to cause reverse plastic failure, which for an undrained test is equivalent to twice the shear strength.

The reloading phase mirrors the unloading with a similar rate of pressure change and eventually crosses the cycle unload path. There are a few points before the main loading path is re-joined because the cycle is not a completely recoverable event.

A chord has been drawn through the start and lowest point of the cycle. The slope of this can be used as a means of calculating shear modulus. If the material response was linear elastic then the result would be the shear modulus. It is apparent that the unloading and reloading data show a non-linear response, and the chord that has been drawn is only the minimum secant. There are an infinite number of steeper secants that could be drawn. The unloading and reloading responses mirror each other and a rotation of the unloading data would describe the same path as the reloading data. This is made explicit in fig 2.6.

2.4 Linear elastic interpretation

If the material response is linear elastic then the local gradient prior to yield can be used as a source of modulus data. In fig 2.1 the part of the curve labelled 'pseudo-elastic' is an example. Because it occurs at the start of the test it is referred to as the initial shear modulus[1], G_i.

Shear modulus is the quotient of the change of shear stress τ and change of shear strain γ:

$$G = \Delta\tau/\Delta\gamma \qquad [2.1]$$

Shear stress and shear strain are not directly measured by the pressuremeter. In fig 2.4 the axes are radial displacement and radial stress at the cavity wall. If the material is linear elastic then a change of radial stress is equivalent to the change of shear stress (in this example, 244kPa). Displacement needs to be expressed non-dimensionally as strain. The change of current cavity strain ε_c is the change of displacement divided by the radius of the probe at the mid-point of the cycle, in this example 3.566×10^{-3}

Current shear strain at the cavity wall γ_c is twice ε_c, an approximation that is convenient and valid if ε_c is small.

This leads to $$G = \Delta p_c/2\Delta\varepsilon_c \qquad [2.2]$$

The calculation for shear modulus G in fig 4 can be carried out using [2.2] and gives 34.3MPa. As G has been derived from an unload/reload cycle it normally has the subscript G_{ur}. Equation[2.2] can be applied anywhere on the loading curve where elastic data can be

[1] [1]Unfortunately, 'initial' is used in two conflicting senses. In the context of non-linear stiffness "initial modulus" generally refers to the maximum or elastic modulus, which in the case of fig 2.1 is certainly not true.

found. If shear strain is calculated as in the example then it is always current shear strain and [2.2] remains valid for all expansions. The advantage is that shear modulus can be derived from displacements without the need for prior processing to identify a strain origin for the entire field curve.

Fig 2.5 *A linear elastic unload/reload cycle*

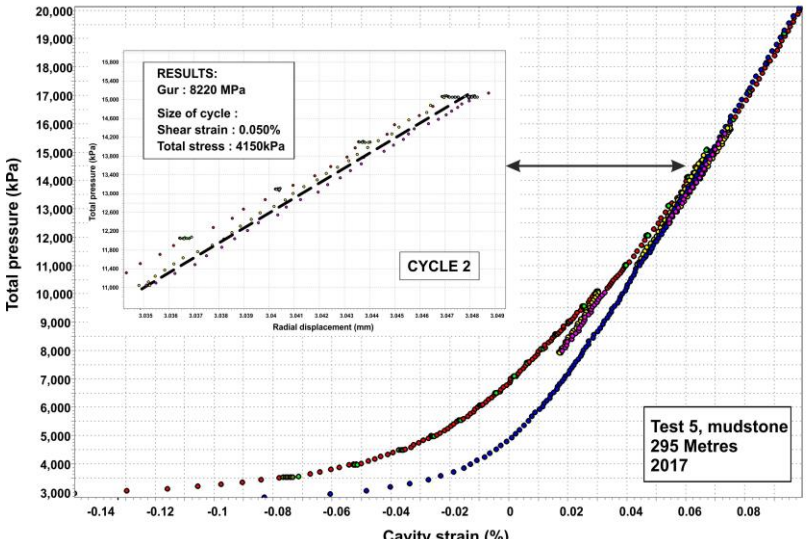

In practice the only material routinely showing a linear elastic response up to the point of yield is intact rock (fig 2.5). There are three such cycles in the test all giving similar results (approximately 8GPa). Because the material is strong enough to support an open hole without failing in the reverse sense, the slope from the latter part of the field curve gives a result similar to the modulus determined from unload/reload data.

2.5 Non-linear stiffness/strain response

In all soils, for shear strains smaller than the yield value, the stiffness/strain relationship is not linear. The unload/reload cycle can be made to give a comprehensive description of this relationship by looking at smaller steps of pressure/strain other than the points at the extreme ends of the cycle. Figure 6 plots the unloading and reloading data from fig 4 in this way. Each path has its own origin, as indicated in fig 4, and the unloading data have been rotated to emphasise that both sets of data are showing the same thing. It follows that it is only necessary to examine one half of the rebound cycle, and the origin for data obtained after the reversal of stress in a loop has the smallest uncertainty because creep is at a minimum (Whittle *et al*, 1992). Fig 2.6 also shows the underlying shear stress response. The test is an undrained event so taking tangents to the radial stress data gives the current shear stress (Palmer ’72, Hughes ’73).

The simplest description of the reloading response is a power law. The exponent of the power law defines the non-linearity of the response and is denoted β. It is generally a number between 0.5 and 1 where 1 indicates linear elasticity. In the example β is almost 0.7, appropriate for a silty clay.

The results in fig 2.6 show the power law trend in radial stress/cavity strain space. Using parameters that the pressuremeter test can determine, this result can be written as:

$$p_c = \eta_h \varepsilon_c^{\beta} \qquad [2.3]$$

η_h is the radial stress constant when the strain scale is current cavity strain (circumferential strain at the cavity wall). Because the test is undrained there are no volumetric strains so shear strain is twice the circumferential strain. This approximation is valid for small strains

below the yielding value. The result in radial stress/shear strain space is given by:

$$p_c = \eta\gamma_c^{\beta} \quad [2.4]$$

where $$\eta = \eta_h/2^{\beta} \quad [2.5]$$

For an undrained expansion, Palmer (1972) shows that the current shear stress τ_c is given by

$$\tau_c = dp_c/d[\ln(\gamma_c)] \quad [2.6]$$

Substituting for dp using the right hand side of [2.4] allows the differential equation to be solved giving

$$\tau_c = \eta\beta\gamma^{\beta} \quad [2.7]$$

Bolton & Whittle refer to $\eta\beta$ as the shear stress constant and call it α. Secant shear modulus G_s is given by :

$$G_s = \alpha\gamma_c^{\beta-1} \quad [2.8]$$

Tangential shear modulus G_t for a shear strain γ is given by (Muir Wood, 1990)

$$G_t = G_s + \gamma_c[dG_s/d\gamma_c] \quad [2.9]$$

Hence from the power law

$$G_t = \alpha\beta\gamma_c^{\beta-1} \quad [2.10]$$

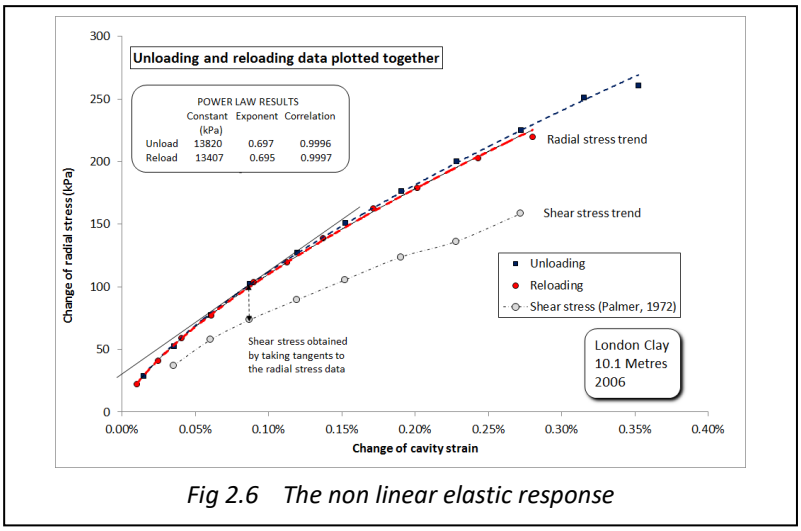

Fig 2.6 The non linear elastic response

[2.8] gives a means of determining the secant shear modulus for shear strains below the yielding value down to 10^{-4}. This is the safe resolution limit of the current generation of pressuremeters and is more than the elastic strain at which the stiffness degradation commences. It is usual to plot the trend between 10^{-4} and 10^{-2} plane shear strain (0.01% to 1%, see figs 2 and 3). Ideally the large strain limit should be the yield shear strain of the material. 1% is appropriate for many stiff clays, but will be too large for sands and too small for soft clay. Secant shear modulus at yield strain is G_y and is the secant shear stiffness governing the pressuremeter loading curve.

It is not necessary to take cycles of small strain amplitude to obtain small strain stiffness parameters. It is better to make the cycles as large as practicable (subject to the condition that the material is not allowed to fail in extension) to obtain parameters from as wide a strain range as possible.

The Bolton & Whittle analysis was developed for undrained tests. For a test in drained material the solution can be used assuming that whilst the material is deforming elastically there are no volumetric strains. Alternatively, the power approach is merely a curve fitting exercise and the solution in radial stress/cavity strain space (equation [2.3]), can be used to generate a smooth data set. This allows a numerical solution for drained tests to be applied (Manassero, 1989). The results are similar to the undrained parameters with a tendency for

β to be slightly higher (more linear). The difficulty is that to apply the drained analysis the ambient water pressure and the constant volume friction angle ϕ'_{cv} must be known or estimated. Figure 2.7 is an example of a test in highly weathered mudstone, with the shear stress/shear strain response obtained by treating a reloading phase as a drained and undrained event. The difference between the two trends will depend on the potential for dilation.

Fig 2.7 Drained & undrained interpretation of the same data

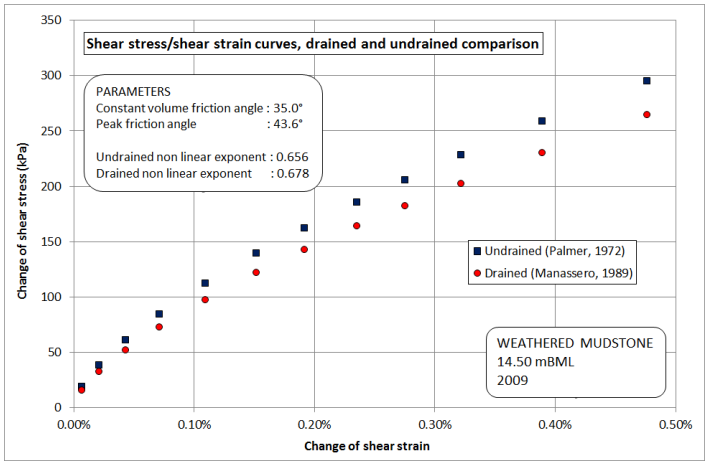

2.6 Stress level

For modulus parameters derived from undrained expansion tests the mean effective stress remains unchanged throughout the expansion and all stiffness/strain data will plot the same trend. Conversely, failure to plot the same trend implies changes in the mean effective stress (fig 2.2).

Whittle & Liu (2013) give a method for both stress and strain adjustment and can be applied to tests that contain at least four unload/reload cycles.

Their solution can be written as: $G = A\sigma^N$ [2.11]

A and N are both semi-log equations incorporating shear strain. For most purposes this level of complexity is not required and a simpler approach can be adopted.

1) Start by carrying out the non-linear analysis described above and discover α and β. Use these to find, for each cycle, G_s at an intermediate value of shear strain, such as 0.1%.

2) Calculate the mean effective stress σ'_{av} at the commencement of each loop.

$$\sigma'_{av} = p'_c/(1+\sin\phi') \quad [2.12]$$

where ϕ' is the peak angle of internal friction

p_c' is the effective radial stress at the cavity wall

p_c' is the pressure measured by the pressuremeter (minus the ambient pore water pressure) and whilst it is increasing σ'_{av} is approximated by [2.12]. This is the mean effective stress at the cavity wall. Houlsby & Schnaid (1994) show experimentally that the stress effect is dominated by conditions immediately adjacent to the pressuremeter surface.

3) Plot modulus against effective stress (fig 2.8).

The example in fig 2.8 shows two tests in sand with multiple unload/reload cycles treated in this way. Each test gives a set of points that follow a power law trend. The exponent of the power law is describing the stress dependency at this level of shear strain. At this strain, typical values for the exponent **n** are in the range 0.3 to 0.4. The correlation coefficient for each trend is better than 0.99.

Fig 2.8 Finding the stress dependency exponent

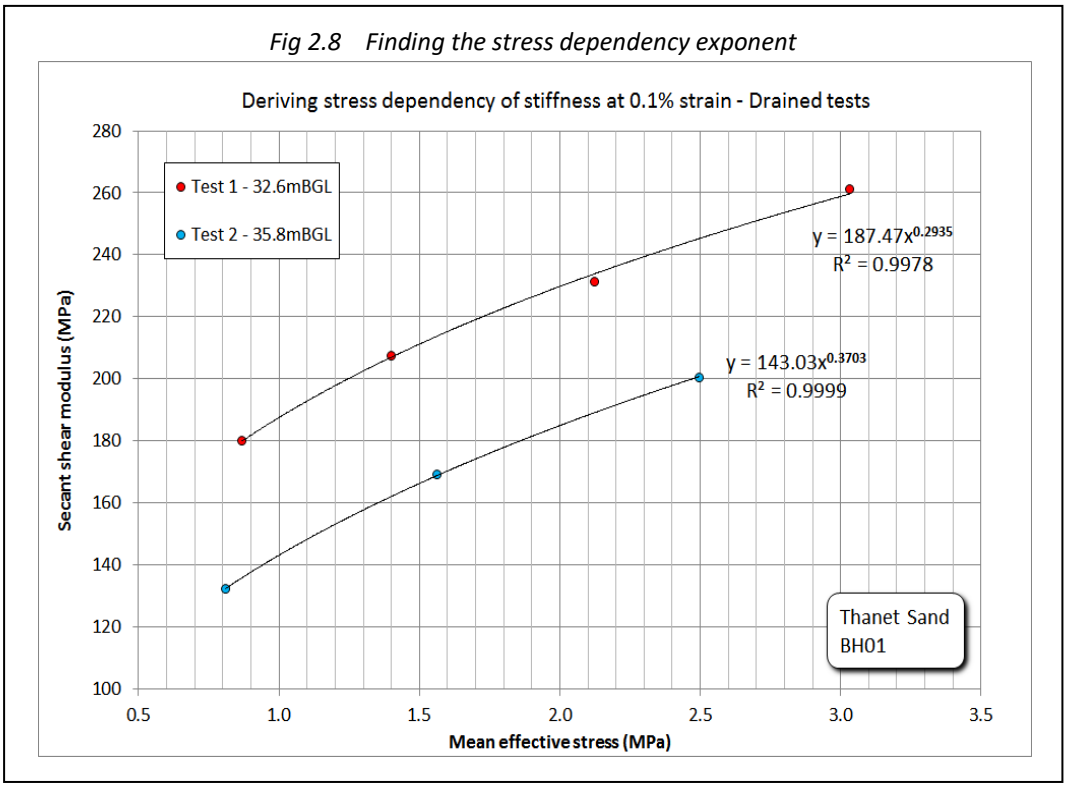

Given the stress dependency exponent, for <u>each</u> cycle a stress adjusted version of α is found, α_{ref}:

$$\alpha_{ref} = \alpha(\sigma'_{ref}/\sigma'_{av})^n \qquad [2.13]$$

[2.13] incorporates the relationship suggested by Janbu ('63) and forms the basis of the approach to stress dependency used in Bellotti et al (1989). The reference stress is typically σ'_{ho}. Once α_{ref} is defined it is used in place of α in [8] to obtain the stress adjusted strain dependent modulus.

Figs 2.9 and 2.10 give a 'before' and 'after' example of the method being applied to a test in dense sand. The scales are the same in both plots, and it is apparent that in practice the stress adjustment gives a trend very similar to that of the first uncorrected cycle. The corrected trend also shows convergence at the strain level used for finding the stress exponent n. This is expected because it is known that the stress adjustment is slightly dependent on strain level. The Whittle & Liu (2013) solution varies n with strain level but for most practical purposes the refinement is not required.

Fig2.9 Uncorrected stiffness/strain data

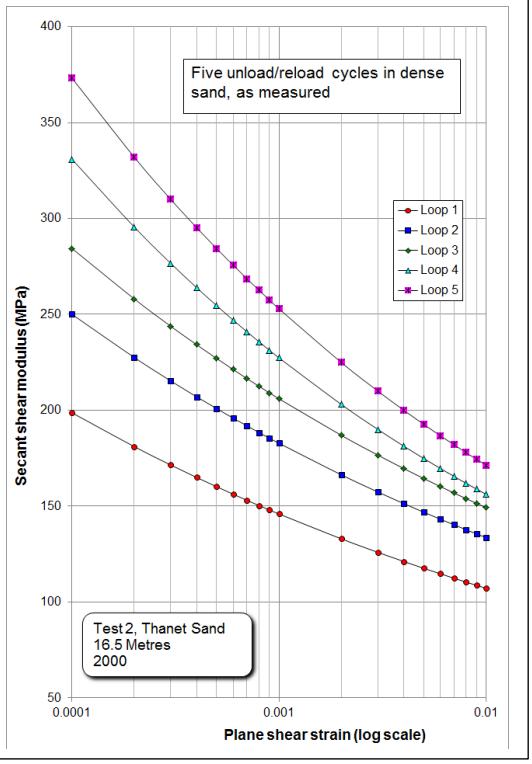

Fig 2.10 Stress adjusted stiffness/strain data

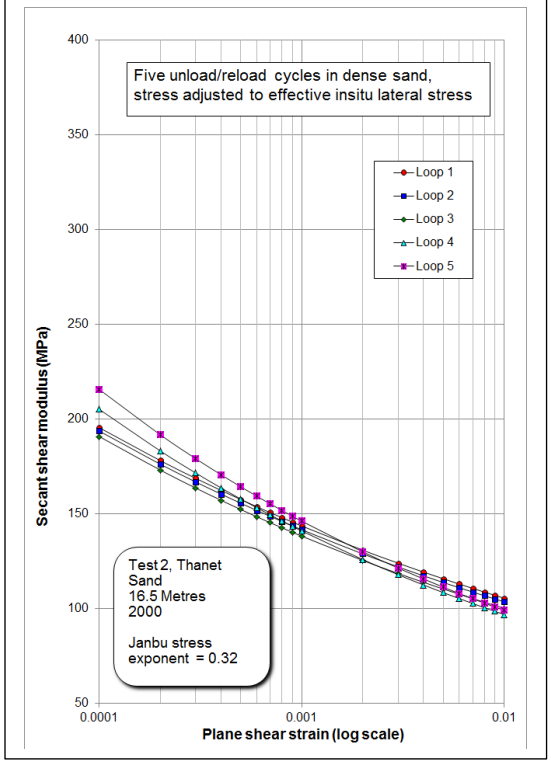

2.7 Cross hole anisotropy

The pressuremeter test gives values for G_{hh}, the shearing stiffness in the horizontal plane. This is directly applicable to the analysis of radial consolidation or cylindrical cavity expansion due to pile insertion. G_{vh} is applicable all shearing which has an element of deformation in the vertical plane, such as under a footing or around an axially loaded pile.

To convert from G_{hh} to G_{vh} some relationship between the two must be assumed. Wroth et al (1979) suggest that anisotropy arises from two causes:

- Structural anisotropy due to the deposition of soil on well defined planes
- Stress induced anisotropy, due to the differences in normal stress acting in different directions.

The second cause implies the stiffness in any direction will be related to the effective insitu stress in that direction, in other words a function of k_o.

It can be shown	$2G_{hh} = E_h/(1+\nu_{hh})$	[2.14]
For undrained expansion	$\nu_{hh} = 1- n/2$	[2.15]
and	$n = E_h/E_v \approx k_0$	[2.16]
From this it follows	$E_h = (4- n)G_{hh}$	[2.17]
and	$E_v = (4- n)G_{hh}/n$	[2.18]

This is as far as an argument from first principles can be taken. k_o is likely to lie between 0.5 and 2, so from [2.16] and [2.17] E_h/G_{hh} lies between 2 and 3.5. From [2.18] E_v/G_{hh} lies between 1 and 1.75.

It is likely that G_{vh} will be linked to E_v by Poisson's ratio in a relationship of the form of [2.14]. Plausible values of E_v/G_{vh} would seem to be 2.4 to 3. Hence in a material with k_o of 2, G_{vh} could be as low as $G_{hh}/3$. Simpson et al (1996) come to the same conclusion, but find in practice heavily over-consolidated London clay approximates to $G_{vh} \approx 0.65G_{hh}$. The influence of the strain range is not separately considered in these studies. Fig 13 shows results from London Heathrow Terminal 5 where the ratio G_{hh}/G_{vh} is ≈1.6. Brosse et al, 2017, report ratios higher than this from four distinct stiff clay soils.

Lee & Rowe (1989) give details of the anisotropy characteristics of many clays varying from lightly over-consolidated to heavily over-consolidated. The general conclusion is E_v/G_{vh} lies between 4 and 5, rather more than the isotropic relationship of 3. They were concerned with the impact of anisotropic stiffness properties on surface settlement so deriving G_{vh} from E_v is unsatisfactory - although G_{vh} is insensitive to the direction of loading, E_v is not.

In all studies, G_{hh} is greater G_{vh}. How much so is not clear, and whether the difference is constant over the non-linear elastic strain range is also not clear

2.8 Shear modulus from other parts of the pressuremeter curve.

The first part of the unloading is an elastic process and can be used as a source of stiffness information. By the time the pressuremeter unloads, creep strains due to consolidation and rate effects will be large, so there will be a tendency for the initial unloading to be too stiff. If some allowance is made for this, then reasonable estimates of the shear modulus will be obtained.

Curve fitting analyses imply a value for the secant shear modulus at yield. Although this is not likely to be the best way of deriving shear modulus data it is important justification for using such analyses that they can predict this independently measurable stiffness.

2.9 Young's Modulus

All modulus parameters derived from the pressuremeter test are shear modulus G_{hh}. They can be converted to Young's modulus E_h using [2.14].

A non-linear version of [16] is $$E = 2\alpha(1+ \nu)(\sqrt{3}\gamma_a)^{\beta-1} \quad [2.19]$$

Where γ_a is invariant or axial strain: $$\gamma_a = \gamma_c /\sqrt{3} \quad [2.20]$$

[2.19] has the virtue that these results can be compared directly with laboratory derived results which tend to use axial strain.

2.10 Non-linear modulus in terms of shear stress

For some applications it is convenient to derive stiffness values as a proportion of the mobilized strength. If the shear strength c_u or shear stress at first failure τ_f is known, and *z* represents the proportion of strength used, then the shear strain γ_z for this proportion is given as follows:

Where $0 < z \leq 1$ $$\gamma_z = [zc_u/\alpha]^{(1/\beta)} \quad [2.21]$$

For example it is common to require G_{50}, the shear modulus when half of the available strength is mobilised. It is straightforward to apply the preceding non-linear stiffness expressions to derive the relevant modulus:

Generally, shear modulus at strength fraction z: $$G_z= \alpha[zc_u/\alpha]^{(\beta-1)/\beta} \quad [2.22]$$

Specifically, for G_{50}: $$G_{50}= \alpha[c_u/2\alpha]^{(\beta-1)/\beta} \quad [2.23]$$

τ_f can be used in place of c_u for tests in drained materials. It will be approximately $p'_o \sin\phi'$ where p'_o is the effective cavity reference pressure and ϕ' is the angle of internal friction.

2.11 Possible method for estimating G_{max} and the threshold elastic shear strain.

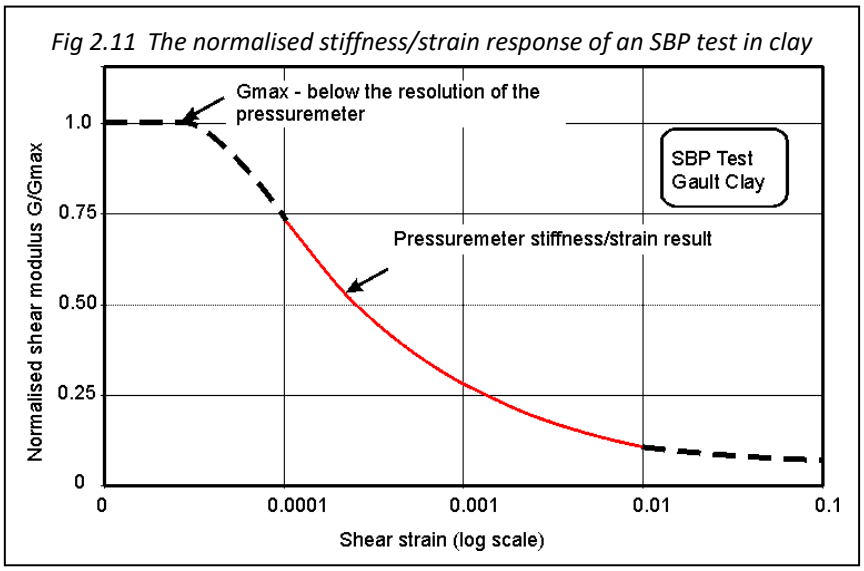

Fig 2.11 The normalised stiffness/strain response of an SBP test in clay

The Bolton & Whittle (1999) procedure is valid for shear strains in the range 10^{-4} to the material yield strain. The lower limit is partly due to the mechanical limitations of the strain measuring devices (residual friction) and partly because the decay curve is a power law which would predict infinite stiffness unless a threshold strain can be specified. Figure 2.11 was drawn using data from an self bored pressuremeter test in Gault Clay, with the part of the curve in red indicating the information provided by a pressuremeter unload/reload cycle.

The full stiffness decay curve is often described with a modified hyperbolic function. Oztoprak & Bolton (2013) use the following to model the decay curves for a wide range of tests conducted in sand:

$$\left(\frac{G}{G_{max}}\right) = 1 \Big/ \left[1 + \left(\frac{\gamma - \gamma_e}{\gamma_{ref}}\right)^m\right] \qquad [2.24]$$

Where G is secant shear modulus at a shear strain γ

γ_e is the shear strain at the elastic threshold

γ_{ref} is the reference shear strain when $G/G_o = 0.5$

m controls the curvature of decay

There is nothing specific to sand about [2.24] apart from the curvature parameter *m*. Oztoprak & Bolton found that *m*=0.88 (in their paper this parameter is denoted *a* but to avoid confusion is here called *m*) gave the best average fit to their database of sand tests. It is reasonable to suppose that the curvature is related to particle size and will therefore vary with soil type.

γ_e is used in [2.24] only to give a constant value for G_{max} at strains less than the threshold strain and can be omitted without significantly affecting the results. Vardanega & Bolton (2013) use this simpler version to describe the decay curves of a database of laboratory tests in fine grained material.

Fig 2.12 Matching hyperbolic and power curves

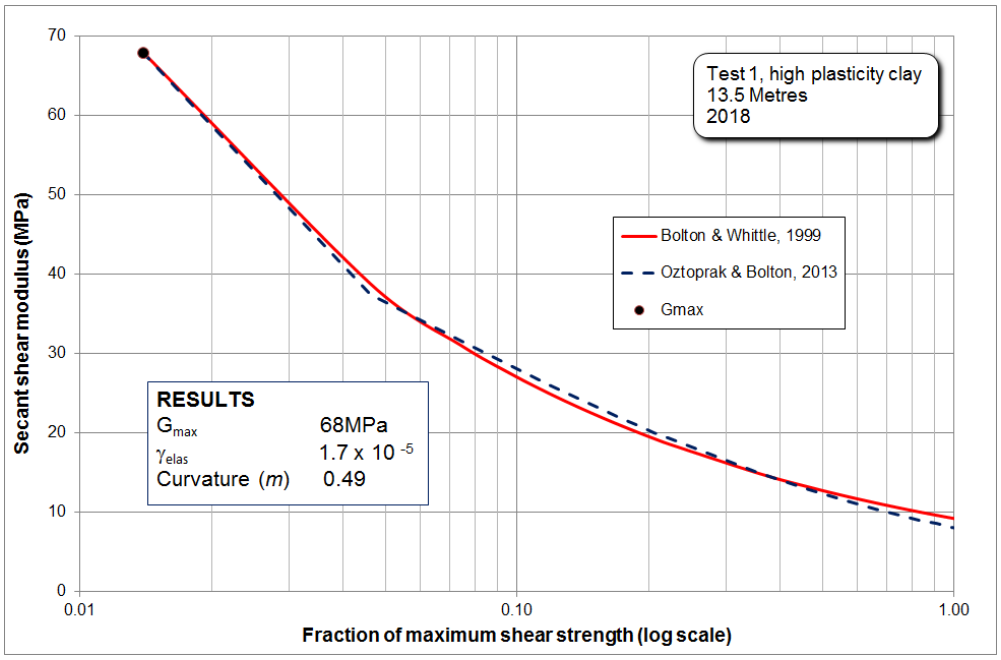

For the pressuremeter test with unload/reload cycles the majority of the stiffness decay relationship is known but G_{max} is not. This invites an iterative approach where successive estimates of G_{max} can be used in [24] to find a modified hyperbolic trend that reproduces the pressuremeter decay data (fig 2.12). The horizontal axis is proportion of mobilised shear stress using [2.22] to relate shear strain to mobilised shear stress. A re-arrangement of [8] is used to find the reference shear strain γ_{ref} and threshold shear strain γ_{elas} whenever the estimate of G_{max} is altered.

Fig 2.13 Comparing laboratory & pressuremeter results for G_{max}

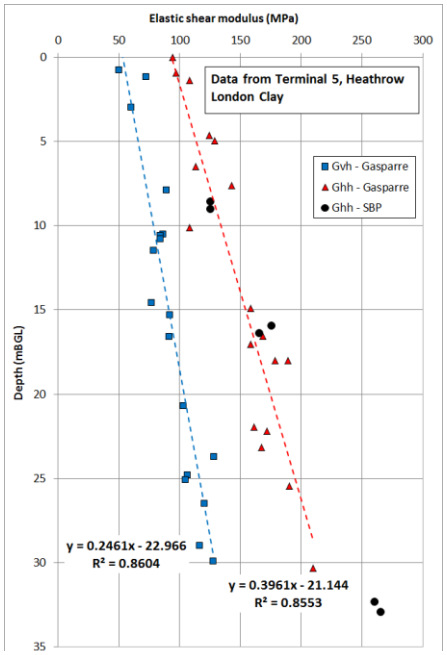

To produce the trend in fig 2.12 the hyperbolic curvature parameter *m* has to be chosen in addition to making estimates of G_{max}. Results suggest *m* is about 0.5. This does not agree with Vardanega & Bolton who report curvature values on average slightly greater than 0.7 but with considerable scatter.

This speculative procedure has been applied to a number of sites and varying materials using different pressuremeter types. The factor *m* is a number possibly calculable from the non-linear elastic exponent, β. The correlation coefficient between data sets predicted by the power law parameters and the hyperbolic parameters is generally greater

than 0.995. There is little judgement involved in setting G_{max} – it is merely adjusted until the correlation coefficient reaches a peak.

Figure 2.13 is an example, comparing high quality laboratory derived small strain stiffness results (Gasparre et al, 2007) with those obtained from self bored pressuremeter tests at the same site.

2.12 Normalisation

The choice of normalisation parameter depends on the underlying purpose. Generally it is the need for a non-dimensional version of a data set where the influence of depth has been removed. In the case of a pressuremeter test the usual choices are the initial effective stress p'_o or strength, typically undrained shear strength c_u in the case of data from tests in fine grained material. A less commonly used though potentially more logical parameter is the effective yield stress, p'_y, which combines both and has an inherent link to the over consolidation ratio. An example of all these methods applied to a reasonably continuous profile of pressuremeter tests is given in Fig 14.

Fig 14 Normalising stiffness/strain data

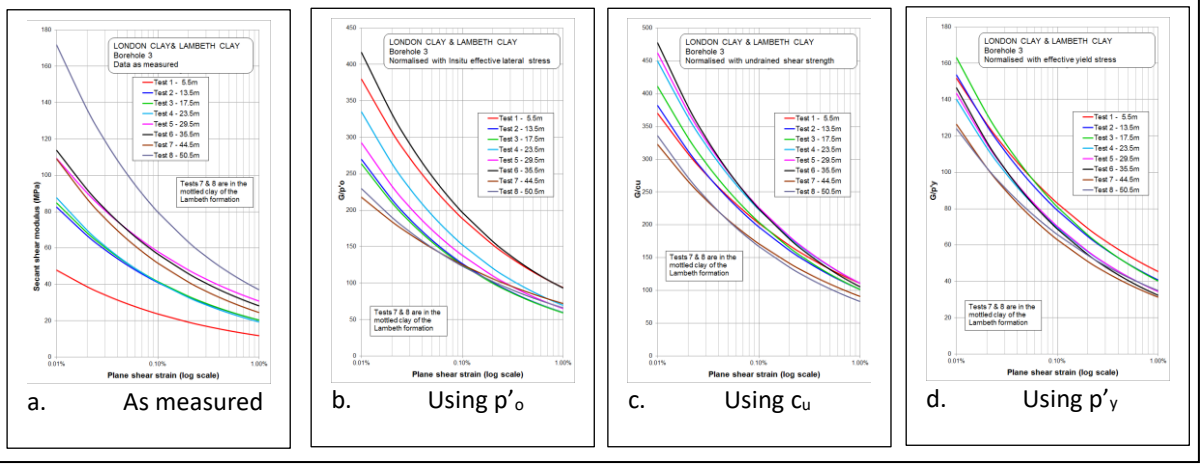

There are eight tests in the example distributed between 5 and 51 metres below surface. The first six are in London Clay, the last two in the heavily over-consolidated mottled clay of the Lambeth Formation. The data as measured has a range of about 3.5, with clear indications of the material boundaries. Fig 14d has a distribution of less than 1.3 with only the Lambeth tests distinguishable from the remainder.

2.13 The limit of recoverability

The reduction of stiffness with increasing shear strain is generally attributed to the loss of inter-granular contact or slippage (Oztoprak & Bolton, 2013) so that within an assembly of particles a growing proportion can no longer make an elastic contribution. This is a recoverable process if the direction of loading and hence straining is reversed and contacts once more engage.

As indicated in fig 2.4, although the unload/reload cycle is almost recoverable there is a small loss which may be attributable to fracture damage occurring at the micro-scale. There is some evidence for this. Although not obvious in figs 2.2 and 2.3, successive cycles tend to show a slight increase in non-linearity which may be attributed to a greater proportion of smaller fragments as breakage progresses. This is not the case for all materials. There are tests where non-linearity either stays constant or even reduces slightly as the expansion continues (fig 2.15). The material in this example has been transported a considerable

distance in fast flowing water, a tumbling process that removes asperities. The more the particles resemble spheres the less likely it is for micro-fracturing to occur as there are fewer opportunities for differential fracture development.

Note that the points obtained by taking tangents directly show stress reduction at larger shear strain. The strain scale extent is arbitrary; what the measured data are indicating is the yield strain of the material.

Fig 2.15 – Reducing non-linearity in a fluvial sand

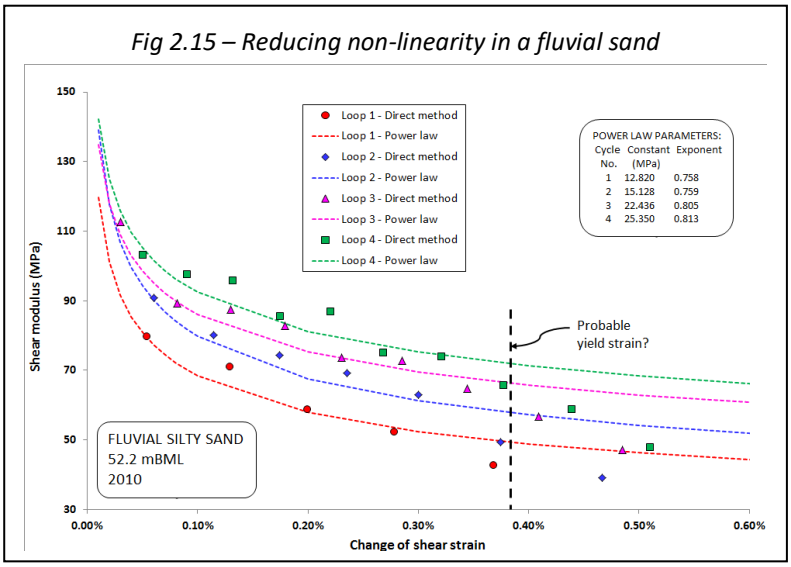

There are situations where it is difficult to make a successful unload/reload cycle. Chalk is an example. Once the yield stress of the chalk has been exceeded there is a tendency for the structure of the material to collapse, a process that will continue indefinitely and is exhibited as a large creep displacement whenever the loading is paused. Reducing the pressure in an attempt to drop below the current yield surface will often result in cycles that are 'V' formed (fig 2.16). The chord through the cycle has been aligned with the reloading data, which in this case is the conservative option. The only cycle in this test to be relatively free of creep influence is the one on the final unloading. Difficulty with creep is also an influence on pushed tests, where the radial stress is approaching the limiting condition.

Fig 2.16 – Effects of creep

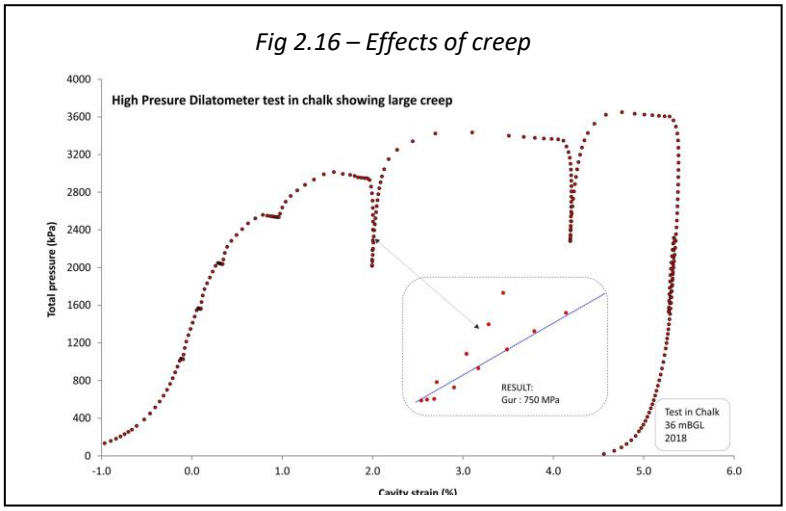

2.14 References for modulus

BELLOTTI, R., GHIONNA, V., JAMIOLKOWSKI, M., ROBERTSON, P. and PETERSON, R. (1989).
Interpretation of moduli from self-boring pressuremeter tests in sand. *Géotechnique* Vol.**39**, no.2, pp.269-292.

BOLTON M.D. and WHITTLE R.W. (1999)
A non-linear elastic/perfectly plastic analysis for plane strain undrained expansion tests. *Géotechnique* Vol. **49**, No.1, pp 133-141.

BROSSE, A., HOSSEINI KAMAL, R., JARDINE, R.J. and COOP, M.R (2017)
The shear stiffness characteristics of four Eocene-to-Jurassic UK stiff clays. *Géotechnique* **67**, **3**, 242-259.

GASPARRE, A., NISHIMURA, S., MINH, N.A., COOP, M.R. & JARDINE, R.J (2007)
The stiffness of natural London Clay. *Géotechnique* **57**, **1**, 33-47.

HOULSBY, G.T. & SCHNAID, F. (1994)
Interpretation of shear moduli from cone pressuremeter tests in sand. *Géotechnique* **44**, **1**, 147-164.

HUGHES, J.M.O. (1973).
An instrument for in situ measurement in soft clays, PhD Thesis, University of Cambridge

HUGHES, J.M.O. (1982)
Interpretation of pressuremeter tests for the determination of elastic shear modulus. *Proc.Engng Fdn Conf. Updating subsurface sampling of soils and rocks and their in-situ testing, Santa Barbara,* pp 279-289.

JANBU, N. (1963)
Soil compressibility as determined by oedometer and triaxial tests*. Proc. 3rd Eur. Conf. Soil Mech*., Wiesbaden 2, pp 19-24.

JARDINE, R.J. (1992)
Nonlinear stiffness parameters from undrained pressuremeter tests. *Can. Geotech*. **29**, pp 436-447

LEE, K.M. AND ROWE, R.K. (1989)
Deformations caused by surface loading and tunnelling: the role of elastic anisotropy. *Géotechnique* **39***,* **1**, 125-140.

MANASSERO, M. (1989)
Stress-Strain Relationships from Drained Self Boring Pressuremeter Tests in Sand. *Géotechnique* **39**, No.2.

MUIR WOOD, D. (1990)
Strain dependent soil moduli and pressuremeter tests. *Géotechnique*, **40**, pp 509-512.

OZTOPRAK, S. & BOLTON, M. D. (2013)
Stiffness of sands through a laboratory test database *Géotechnique* **63**, No. 1, pp 54–70

PALMER, A.C. (1972)
Undrained plane-strain expansion of a cylindrical cavity in clay: a simple interpretation of the pressuremeter test, *Géotechnique* **22** No. 3 pp 45l-457.

SIMPSON, B., ATKINSON, J.H. AND JOVICIC,V. (1996)
The influence of anisotropy on calculations of ground settlements above tunnels. Proc. Int. Symp. Geotechnical aspects of Underground Construction in Soft Ground, City University, London, April.

VARDANEGA P. J., AND BOLTON M. D. (2014)
Stiffness of Clays and Silts: Normalizing Shear Modulus and Shear Strain. *J. Geotech. Geoenviron. Eng. 2013.139:1575-1589.*

WHITTLE R.W (1999)
Using non-linear elasticity to obtain the engineering properties of clay. *Ground Engineering*, May, vol. 32, no.5, pp 30-34.

WHITTLE, R.W. , DALTON, J.C.P. , HAWKINS P.G. , (1992)
Shear Modulus and Strain Excursion in the Pressuremeter Test*. Proc. Wroth Memorial Sym*., Oxford, July 1992.

WHITTLE R.W and LIU LIAN (2013)
A method for describing the stress and strain dependency of stiffness in sand. *Proc. ISP6, Paris, 2013*

WROTH, C.P. (1984)
The Interpretation of In Situ Soil Tests. Twenty Fourth Rankine Lecture, *Géotechnique* **34**, No. 4, pp 449-489

WROTH C.P., RANDOLPH M.F., HOULSBY G.T. AND FAHEY M. (1979)
A review of the engineering properties of soils with particular reference to the shear modulus. *Cambridge University Engineering Department, Soils TR75.*

ANALYSING CYLINDRICAL CAVITY LOADING TESTS

PART 3 ANALYSES FOR INSITU LATERAL STRESS

3 ANALYSES FOR INSITU LATERAL STRESS

3.1 Overview

The expansion pressuremeter test is a sequence of measured co-ordinates of pressure and displacement of the cavity wall (once suitable corrections have been made to compensate for the response of the elastic membrane). Analyses that extract the stress/strain properties of the ground from the pressure/displacement data need to know the start point, the initial stress and displacement to which subsequent measurements are referred. The initial stress, the Insitu lateral stress σ_{ho} is particularly difficult to identify. It is more usual to refer to a cavity reference pressure p_o which may be synonymous with σ_{ho}. The initial radius, r_o in fig 3.1, is possibly more obvious.

Although in principle the stress ordinate of the initial radius ought to be p_o, in practice this cannot be the case unless the probe has been inserted into the material with insignificant disturbance. However assuming the two values are co-incident is the starting assumption.

For insertion methods that imply stress *relief*, the origin is taken to be the point where the cavity is restored to its original or reference condition. A reference stress, p_o, is identified that seems to represent the point at which the cavity begins to expand. The displacement ordinate of this stress (r_o in fig 3.1) is used to convert subsequent displacements to strain.

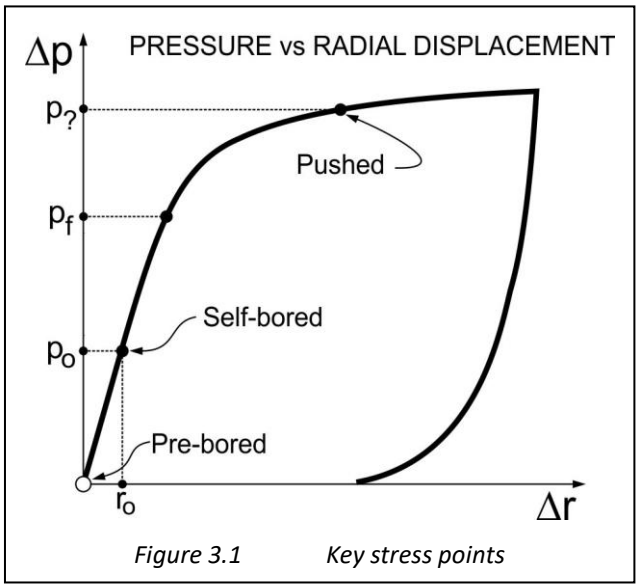

Figure 3.1 Key stress points

Fig 3.1 is showing a 'perfect' pre-bored test. For a similarly 'perfect' self -bored test the expansion will not commence until the applied stress reaches p_o , allowing the cavity reference stress to be identified by inspection. This is the so-called 'lift-off' method.

The self boring pressuremeter is fitted with pore pressure transducers, and the trend of excess pore water pressure against total stress can be used to identify yield stress and reference stress.

It is also possible to recognise by inspection the shear stress limit (the point marked p_f in Figure 3.1) as this is indicated by the onset of a markedly non-linear response. An iterative procedure first suggested by Marsland & Randolph (1977) allows p_o to be inferred. The published method is not valid for tests in sands and tests in material with non-linear elastic properties. This effectively rules out all soils. Nevertheless it is usual to apply the procedure because it tends to set an upper limit to any estimate of reference stress.

Elements of these methods are outlined in Mair & Wood (1987). For a pushed test, the expansion commences when the material is already in a plastic state, $p_?$ in fig 3.1. The question mark indicates that although the pressure can be seen, the radial displacement ordinate cannot be used as part of a meaningful strain calculation.

A more novel approach is the balance pressure creep method (Hoopes & Hughes, 2014). This is a procedure that examines in close detail the latter stages of the final contraction. A

small reload/unload event is carried out where the steps of pressure are held constant and the magnitude and direction of any time-dependent movement are identified. There is a possible null stress for which there is no discernible movement either inwards or outwards and this 'balance pressure' is assumed to be the geostatic lateral stress. Potentially, this gives a means of means of obtaining reference stress estimates for all types of pressuremeter, no matter how disruptive the insertion process.

Some rigour can be applied to all these procedures by using the full set of parameters derived from a pressuremeter test within a closed form model to discover whether the measured field curve can be recovered. The input data set is then adjusted in a controlled manner until the best match for all parameters is obtained. In certain models (Whittle, 1999) the only free parameter is the reference stress.

Apart from the balance pressure creep method, modelling may be the only means of obtaining a reference stress by analytical methods from an undrained pushed test (Houlsby & Withers, 1988).

In all cases what is determined is cavity reference pressure, p_o. It is not possible to measure the insitu lateral stress σ_{ho} because the act of placing instrumentation always results in some movement, even if very small, and movement means a change in stress. Due to the non-linear nature of soil stiffness a movement of a few micro-strain can result in a large stress alteration. The methods above are indirect indicators for determining σ_{ho}. It is open to question whether p_o is equivalent to σ_{ho}, and multiple sources are examined in order to decide if the assumption is plausible . External evidence might take the form of using the derived reference stress within a k_O calculation, or checking that the derived vertical/horizontal anisotropy can be supported by the material shear strength:

$$\sigma_{ho} - \sigma_{vo} < 2C_u \; . \qquad \ldots[3.1]$$

In practice there is a wide range of values that would satisfy this condition so its usefulness is limited.

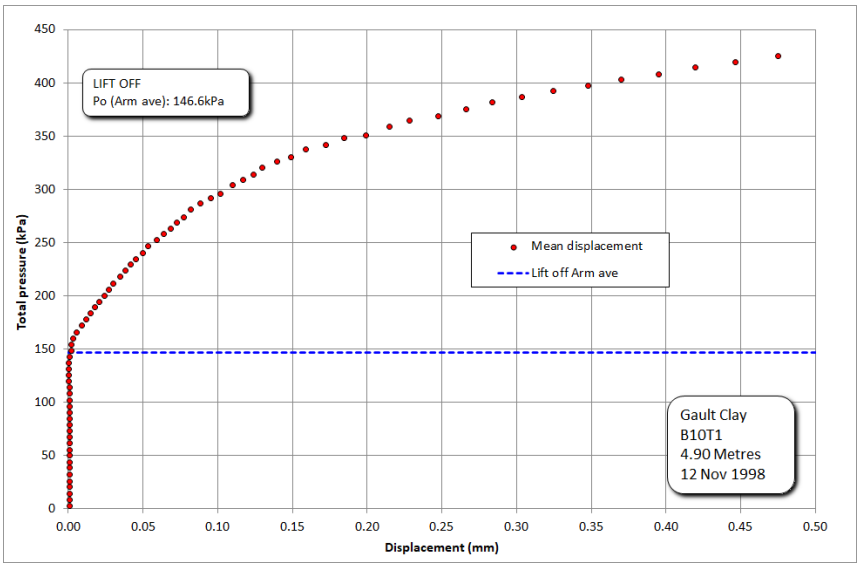

Fig 3.2 An example of lift-off

3.2 Lift-off

This method ought to be applicable only to the relatively low disturbance self-bored test, but occasionally it seems to give sensible results with more extreme insertion procedures. In principle it is straightforward. The instrument is assumed to be bored into the ground with insignificant disturbance caused to the surrounding material. If the insitu conditions around the instrument remain unchanged by the insertion process then the pressure at which the

membrane first moves and the cavity begins to expand is p_o. The corresponding cavity diameter will be the same as the at rest diameter of the instrument. Because the initial part of a self-bored test is very stiff the choice is made from an enlarged view of the first 0.5mm (≈1.2% cavity strain) of the expansion (fig 3.2). This range is sufficient to show any elastic behaviour and the early stages of the expansion post-yield.

Difficulties arise because the instrument has finite stiffness and hence there is instrument compliance to be separated from the expansion of the cavity. At the start of the test when the internal pressure is ambient the instrument is being externally loaded by the lateral stress in the ground. This external stress is forcing the displacement followers inwards so unless the seating of the followers at the zero state is perfect there will be a stored error movement. At the point where the internal pressure matches the external stress these imperfections are revealed as a characteristic 'signature' for the individual arms. In a simplistic approach these signatures could be considered as positive indications of the reference pressure. However in the ground it is not possible to have displacements without an associated change in stress, which add to or subtract from the reference pressure.

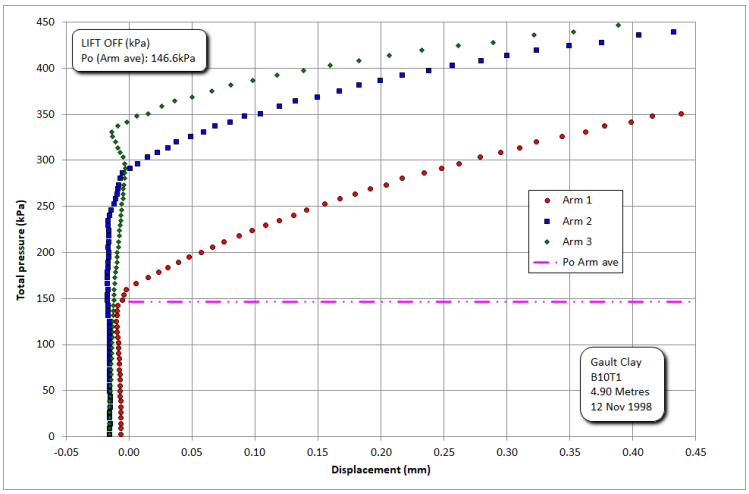

Fig 3.3 Lift-off, all arms shown

As a consequence of these error effects, applying the lift-off analysis means that there can be considerable uncertainty attached to identifying a plausible reference pressure. Conventional practice for coping with this uncertainty is to relax the definition of 'lift-off' to mean something more like 'significant movement'.

Figure 3.3 is an illustration of the problems involved with identifying lift-off. Here the individual arms from the SBP test in fig 3.2 are plotted. There are many choices of lift-off stress depending on how rigorous the interpretation of what is implied by the term. In general the strict lift-off stress is that obtained from the first arm to move. The variation in the starting stress distribution indicates defects in the installation process. The probe may not be perfectly vertical, or may not be removing material efficiently enough to avoid raising the local state of stress in material immediately adjacent to the pressuremeter.

It is important to bear in mind the scale. The lift-off information is concentrated into the first 100 micrometres of the expansion or about 0.25% cavity strain. This is less than the strain required to make the material reach the fully plastic condition (yield). Because the movements are well within the elastic range of the material the analyst is justified in attributing significance to the output of the separate arms. In this event the arithmetic mean of the separate lift-off points can be a more useful parameter than lift-off derived from averaged arm displacement data.

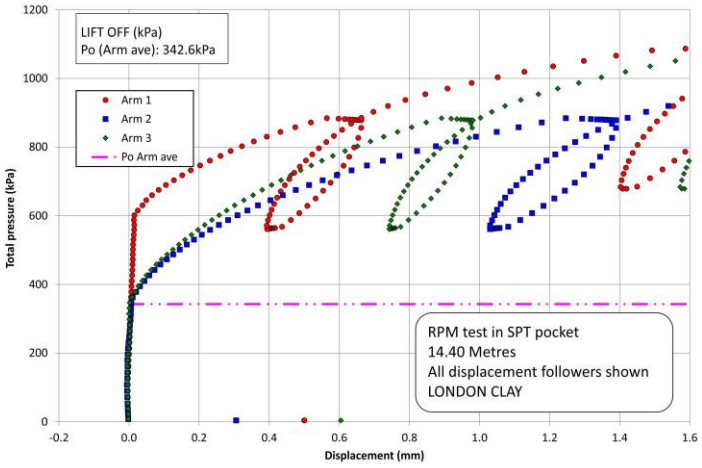

Fig 3.4 Lift-off in a pushed RPM test

If a strict definition of 'lift-off' could reasonably be applied then no assumptions concerning soil response are required. In the less rigorous application that in practice is followed most of the time, it is important that the analyst identifies the onset of plastic behaviour as a guide to deciding that some conspicuous change of form in the loading curve at a lesser stress is likely to be p_o. Plots would still refer to such a break point as 'lift-off' but clearly it is something else, p_o by inspection perhaps.

Fig 3.4 is an extreme example. This is an extract from an RPM test made in a pocket formed by SPT tools. The material has been grossly disturbed by the SPT and has probably been taken to near limit conditions before the pressuremeter is positioned. Nevertheless there are clear examples of 'lift-off' stress. It happens for this test that the best-estimate for p_o is 290kPa rather than the lift-off value of 343kPa but under the circumstances this is acceptable ball-park agreement. It is possible that the influence of the lateral geostatic stress results in a stress witness in the measured response even under conditions of major disturbance. It is an area that requires further investigation.

3.3 Marsland & Randolph (1977) yield stress analysis

Marsland & Randolph analysis for undrained soils relies on being able to identify the onset of plastic behaviour, the yield stress p_f. The argument is as follows:

- In the vicinity of the insitu lateral stress the soil response is simple elastic and therefore the total pressure/ cavity strain plot will be linear. Identify this slope (and incidentally, use it calculate the initial modulus G_i).
- Elastic behaviour will cease when the undrained shear strength of the soil is reached in the wall of the cavity, and hence the pressure /strain plot will begin to curve (see fig 3.1).
- The yield stress can be written as:

$$p_f = p_o + c_u \qquad [3.2]$$

- From this it follows that p_o can be deduced by iteration using a plot of displacement against total pressure.
- Initially a guess is made of p_o, such as 50% of the yield stress. The displacement ordinate of the chosen p_o defines an interim origin to convert displacement to strain.
- It is then possible to produce a total pressure:log shear strain plot to find the undrained strength c_u (Gibson & Anderson, 1961).

- The sum of these two parameters is compared with the selected value of p_f. The choice of p_o is then suitably adjusted and the process repeated until a match is found. It is a straightforward matter to carry out this procedure on the computer.

The modified method in current use is a response to the difficulty that perfectly plastic deformation is not a realistic enough model for many materials and yield may occur at a different shear stress than the large strain shear strength. Hawkins et al (1990) suggested that the most appropriate choice was that value of shear stress pertaining at the apparent onset of plasticity, so [3.2] now becomes:

$$p_f = p_o + \tau_f \qquad [3.3]$$

τ_f can be obtained from a total pressure:log shear strain plot by selecting the slope at the

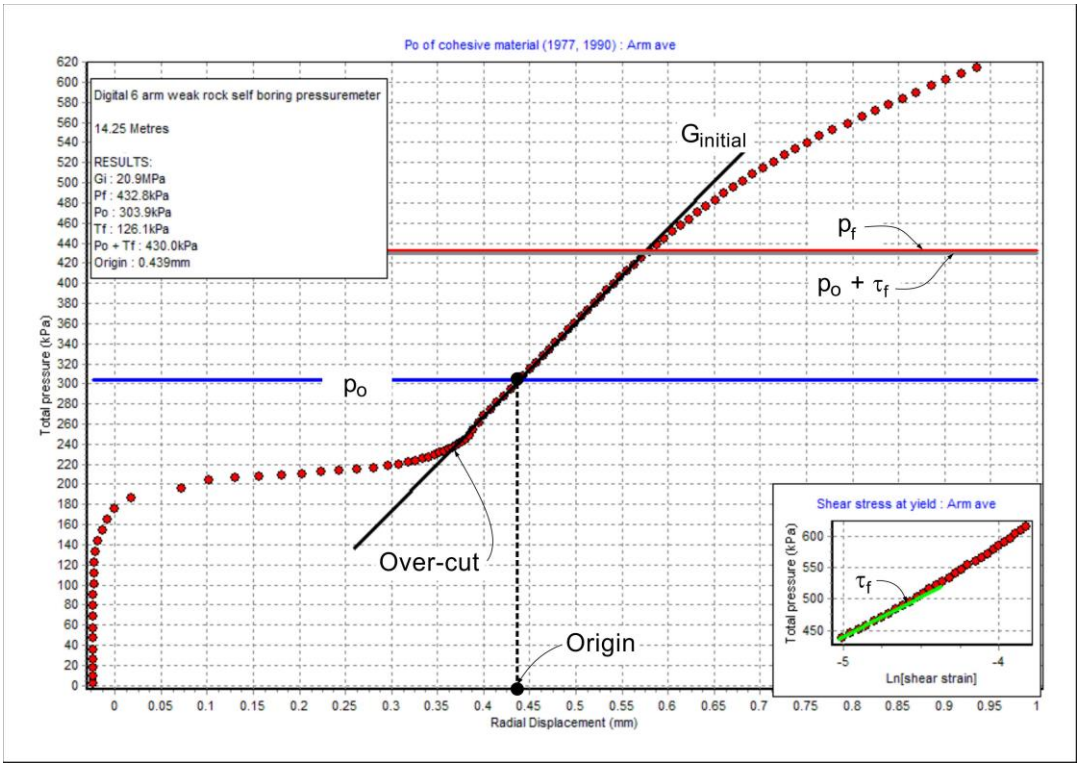

Fig 3.5 An example of the Marsland & Randolph analysis

pressure and strain corresponding to the choice of p_f. In practice this substitutes the Palmer (1972) numerical solution for the Gibson & Anderson solution. See inset plot in fig 3.5.

The analysis is implemented graphically, using rulers to mark significant points on the curve (fig 3.5).

It is necessary to be realistic about what the method can do. In the case of the example above, the test is made with a self boring probe arranged to bore fractionally over-size in a stiff clay. The 0.35mm overcut is very close to the overbore dimension and indicates that the material has not slumped. Under these circumstances, which approximates 'perfect pre-boring' the analysis gives sensible results because any small relaxation can be supported by the available shear strength. Generally, this is not the case.

Figure 3.6 shows a slightly different version of the same analysis applied to a genuine pre-

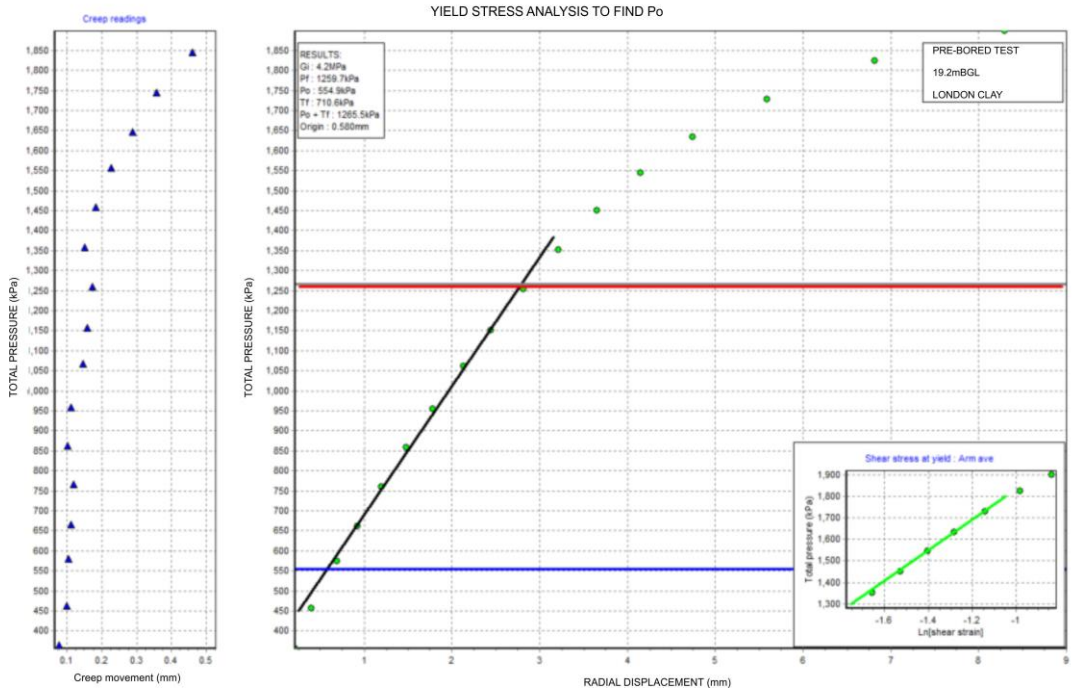

Fig 3.6 *An example of the Marsland & Randolph analysis with creep readings*

bored pressuremeter test. The loading was carried out as a series of pressure steps, each step held for one minute. The plot on the left is the 'creep' movement for each hold. The plot on the right is similar in arrangement as fig 3.5 except that the data are those taken at the end of a creep interval so give an especially smooth curve. The creep readings give an additional indication of the yield stress as there is an acceleration in the movement. It is not quite so easy to detect the cavity reference stress.

The failure condition given in [3.2] could be written:

$$p_f = p_o (1 + \sin \phi') \qquad [3.4]$$

where ϕ' is the peak angle of internal friction

This would make it appropriate for drained tests in purely frictional material such as sand. In place of deciding shear stress from an undrained analysis, a procedure such as Hughes et al (1977) would need to be applied.

Alternatively [3.2] and [3.4] could be combined for a c'- ϕ' material:

$$p_f = c' \cos \phi' + p_o \sin \phi' \qquad [3.5]$$

where c' is drained cohesion

The difficulty is that [3.4] and [3.5] require additional information not directly measured by the pressuremeter test. [3.3] is easily implemented and applied to all stress paths, some of which imply significant compromise. It will not be accurate, but used as a rough guide to the initial stress state, remains useful. However it is unlikely to be the best tool for the purpose.

For one particular circumstance applying the analysis is seriously misleading. This is when the insertion process has raised the initial state of stress, such as a pushed test but also an under-drilled self boring pressuremeter test. In this event the analysis can contribute

nothing – forcing such data to fit the assumptions of the analysis will severely over-estimate the cavity reference pressure.

3.4 Deriving parameters from the excess pore pressure trend

Fig 3.7 The ideal pore pressure response (after Bolton & Whittle, 1999)

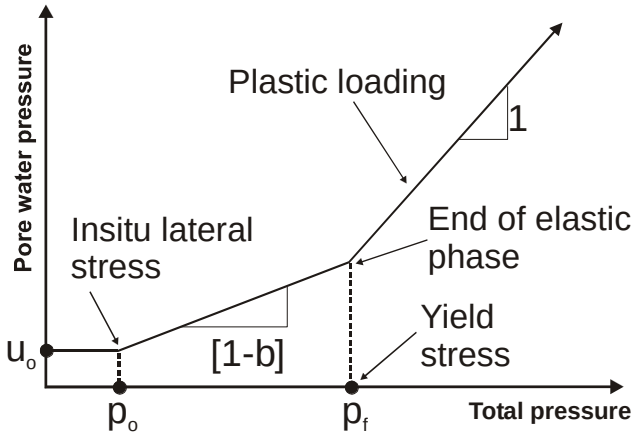

Bolton & Whittle (1999) predict the trend of excess pore water build –up from an undrained cavity expansion in a non-linear elastic/perfectly plastic material (fig 3.7). The significant difference between this trend and that in a simple elastic/perfectly plastic medium is the generation of some excess pore pressure during the pseudo-elastic phase of the test prior to the material fully yielding. The rate at which the pore pressure rises during the elastic phase is related to the exponent of non-linearity, β, a number less than 1 unless the response is truly linear elastic (the Bolton & Whittle analysis is described more fully in Part 4).

In both cases, once the material becomes plastic, there is a 1 for 1 correspondence between

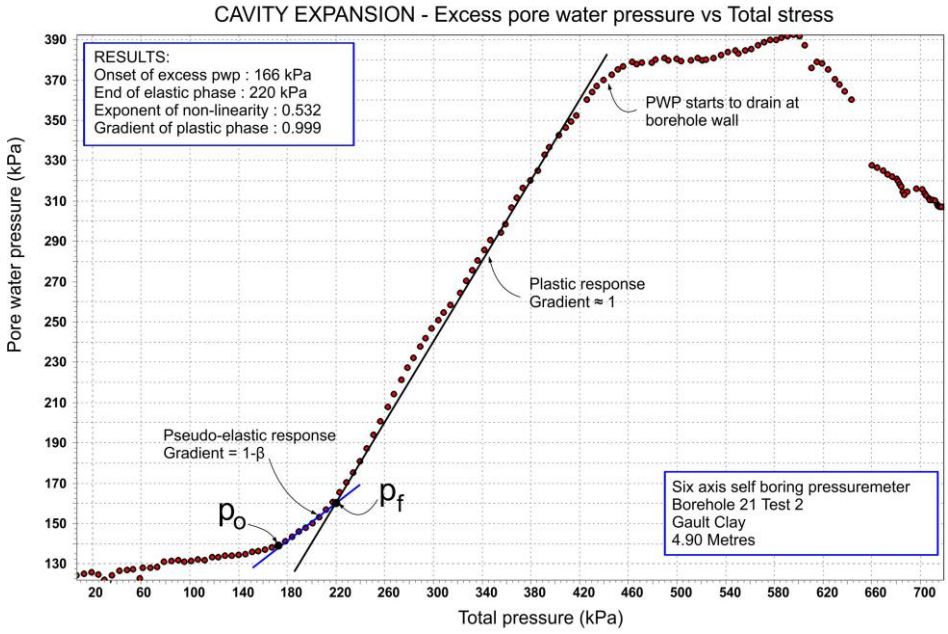

Fig 3.8 An example of pore pressure response

changes in total stress and changes in pore water pressure. In practice, few self boring tests have the necessary minimal disturbance to show the full theoretical behaviour. Even for tests where the insertion procedure is optimal the interruptions to the loading to take unload/reload cycles tend to disrupt the pore water pressure generation.

Fig 3.8 is a typical example of what can be achieved in practice. In the latter stages of the loading when unload/reload cycles are taken the pore water pressure response levels off. This indicates partial drainage, probably not in the soil mass but locally at the borehole wall where gaps in the protective sheath introduce axial drainage paths.

3.5 Deriving insitu lateral stress by curve modelling

The uncertainty in associating a particular value for cavity reference pressure p_o with the insitu lateral stress σ_{ho} can be reduced by curve modelling. Jefferies (1988) is a procedure for deriving insitu lateral stress, stiffness and strength from undrained pressuremeter curves by matching the measured data points with an iteratively selected parameter set. Some rigour is introduced into the procedure by making the set of parameters match the contraction as well as the expansion phases of the SBPM test.

The model used to represent the deformation characteristics of the soil has to be realistic. Jefferies (1988) follows Gibson & Anderson in assuming a simple elastic response until the full shear strength of the material is mobilised and a perfectly plastic response thereafter. Outside of a computer, there is no such soil and the model does not predict the measured field values for stiffness. This is a serious deficiency because it is the one property of the soil that pressuremeters provide reliably without major difficulty.

However the procedure can be used with more representative soil models, and it is customary now to back-analyse undrained tests using a non-linear elastic/perfectly plastic shear stress:shear strain solution. As described in Whittle (1999) this uses as input the already determined values of stiffness and shear strength so the only variable to be decided

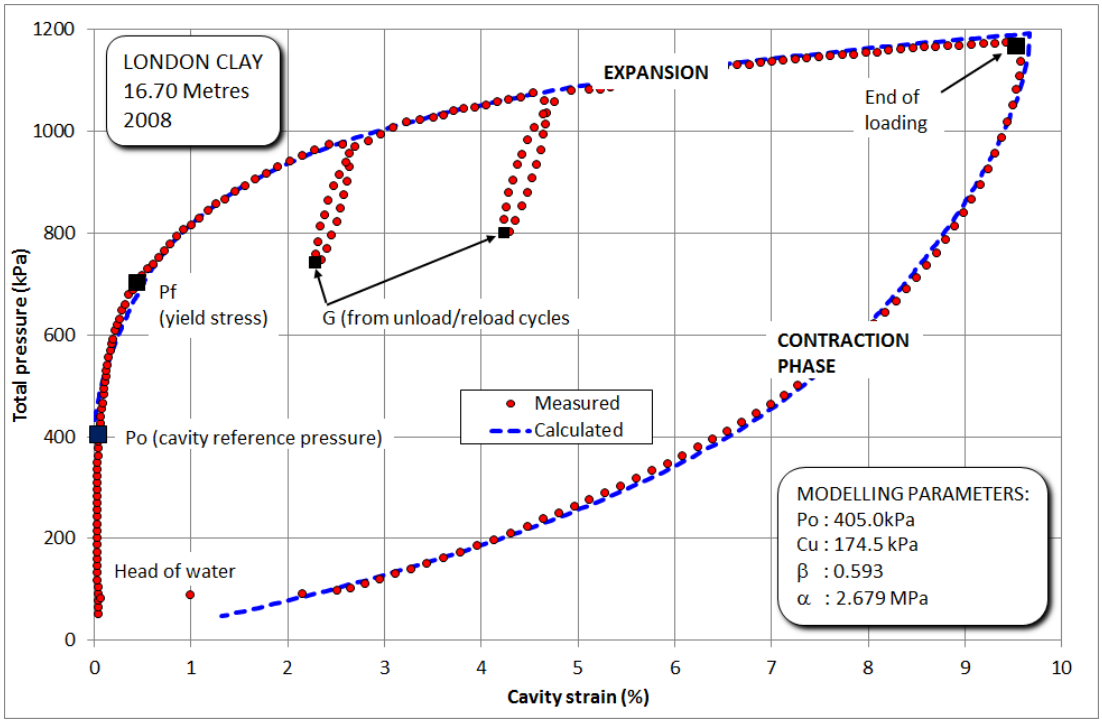

Fig 3.9 Undrained curve fitting example, self bored test

is the insitu lateral stress. Both expansion and contraction phases of the test are fitted (fig 3.9). The model is given in more detail in Part 4.

There are similar methods for drained tests using a non-linear version of the solution suggested by Carter et al (1986). These models are outlined in Part 5.

For a SBP arranged to drill to size, the values for lateral stress derived using the non-linear undrained model are often lower than those obtained by inspection, and are consistent with a view of the test as slightly under drilled. This raises the state of stress around the probe. If the probe is configured to drill fractionally oversize the reverse situation can happen. It is generally easier to interpret an over-drilled test compared to an under-drilled test.

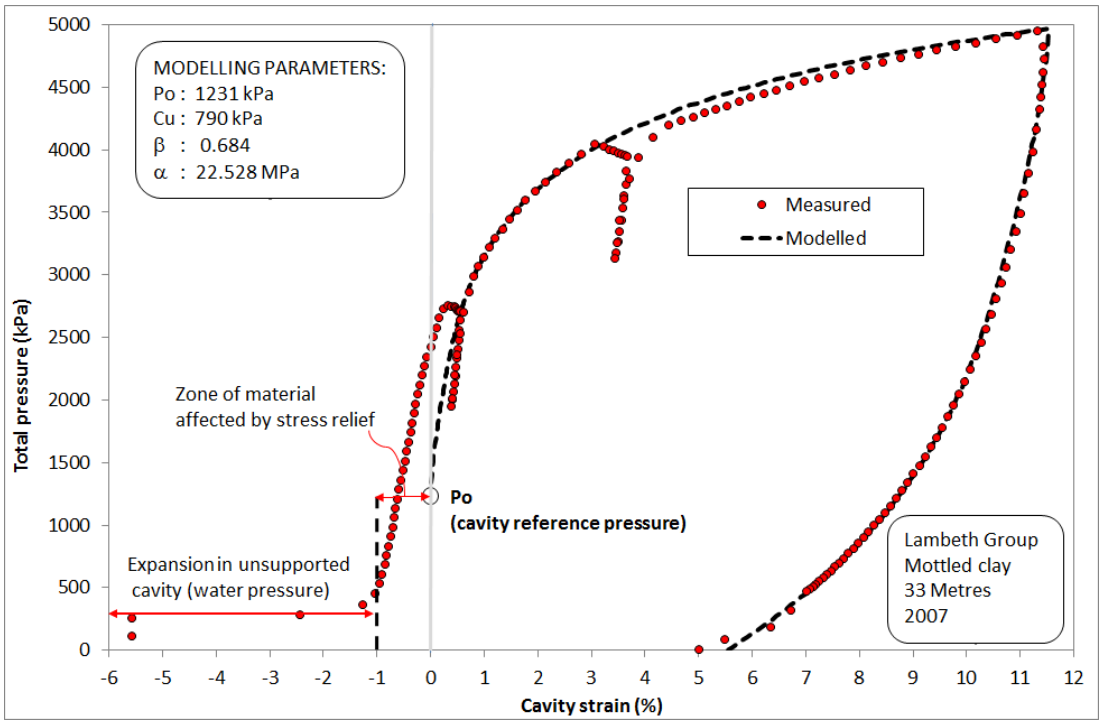

Fig 3.10 Undrained curve fitting example, pre-bored test

The procedure can also be applied to pre-bored pressuremeter test data but the fit to the initial part of the loading will not be possible (fig 3.10).

Only one value for insitu lateral stress is derived using these procedures, as isotropy of soil properties is a fundamental assumption. Because the procedure makes uses of all the evidence it is the preferred method for deriving the insitu lateral stress.

3.6 Balance Pressure Creep Test

The Balance Pressure Creep (BPC) method is outlined in Hoopes & Hughes (2014), and fig 3.11 is an example of a test in clay that includes an implementation of the method. Fig 3.12 shows the BPC part of the test expanded.

The method consists of a series of pressure holds on the final unloading, each hold held for a fixed period. The Authors suggest 2 minutes. The ground response is monitored for indications of the geostatic lateral stress. Inward creep means that the applied stress is below the lateral stress, outward movement means the reverse. It is argued that there is a stress, the balance pressure, where movement will be zero. It is not necessary to apply a pressure hold at the exact point of balance, the pressure steps can be plotted and interpolation used to decide the point of zero creep.

In practice it is more complicated. Creep from this part of the test depends on the direction of loading immediately preceding the hold, where the BPC test is started in relation to the

balance point, and the permeability of the material. For most situations it is not the creep movement but the creep rate that becomes zero at the balance point (fig 3.13).

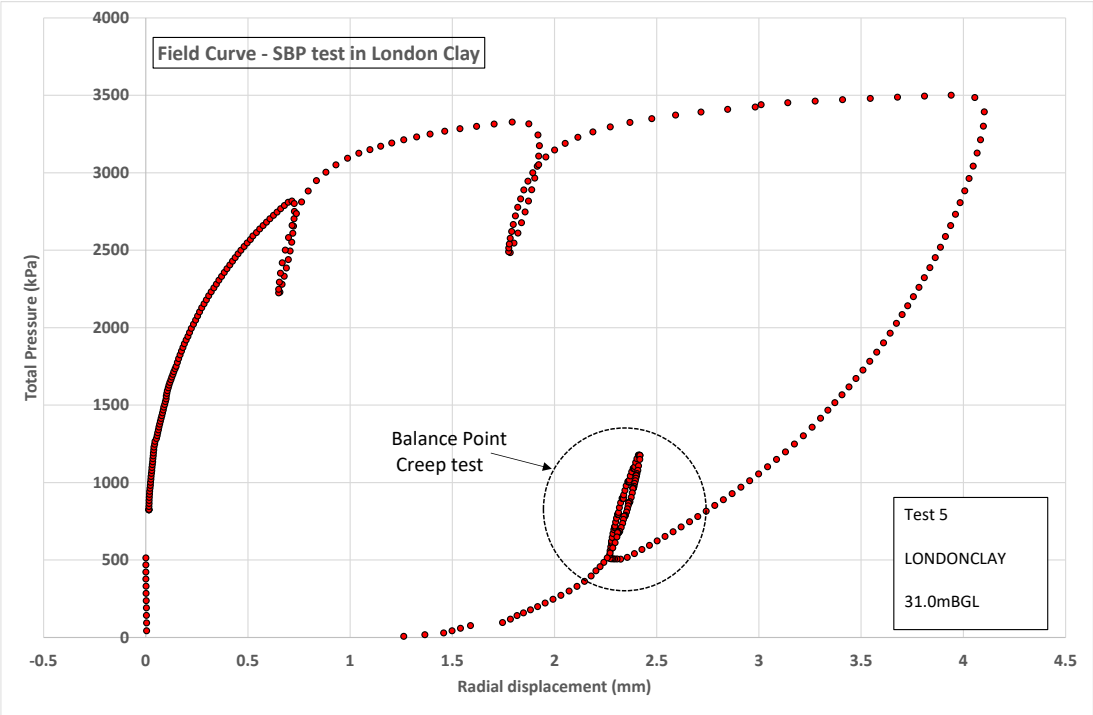

Fig 3.11 SBP test in London Clay that includes a BPC test

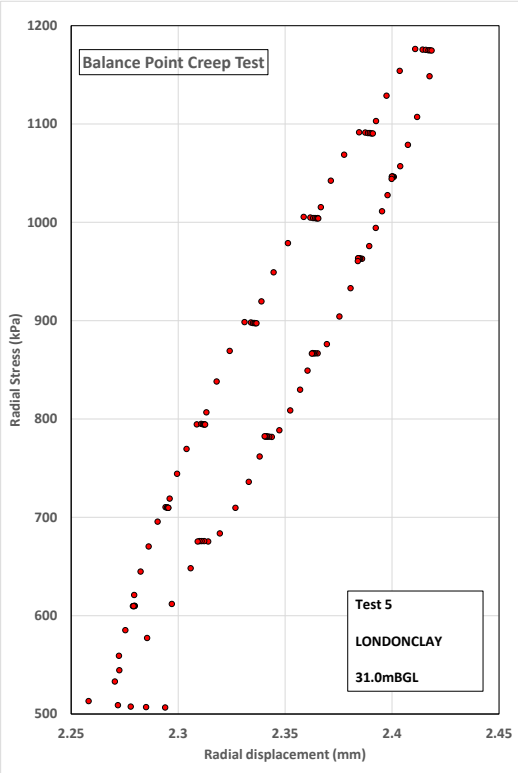

Fig 3.12 Enlarged view of BPC test

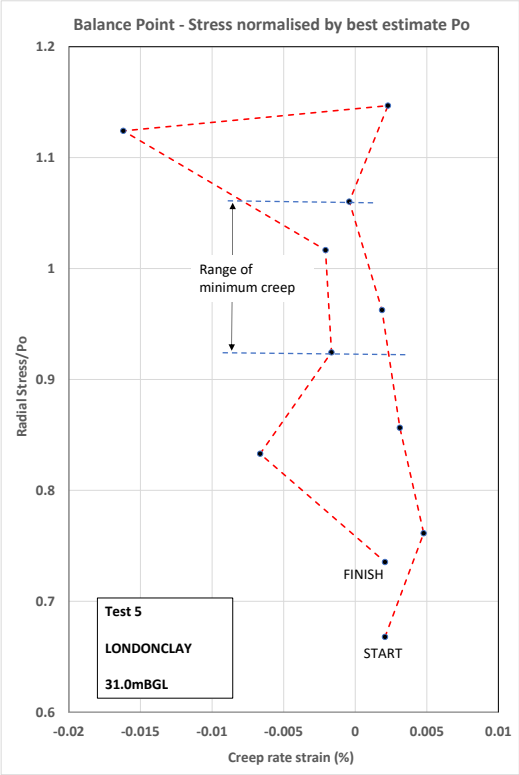

Fig 3.13 BPC analysis

The procedure used in this example is to begin the BPC test at approximately 50% of the over-burden stress and continue it until a stress of twice the over-burden has been applied.

It is expected that in this material this will cover the plausible range for the Insitu lateral stress. There are several holds, both on the loading and unloading arm of the BPC test, but held for a relatively short time of 30 seconds. The start and finish of a holds give a creep displacement for a particular stress and the difference between adjacent steps is plotted in fig 3.13. The stress data have been normalised by the best estimate available for the cavity reference pressure, which in this case was decided by curve modelling.

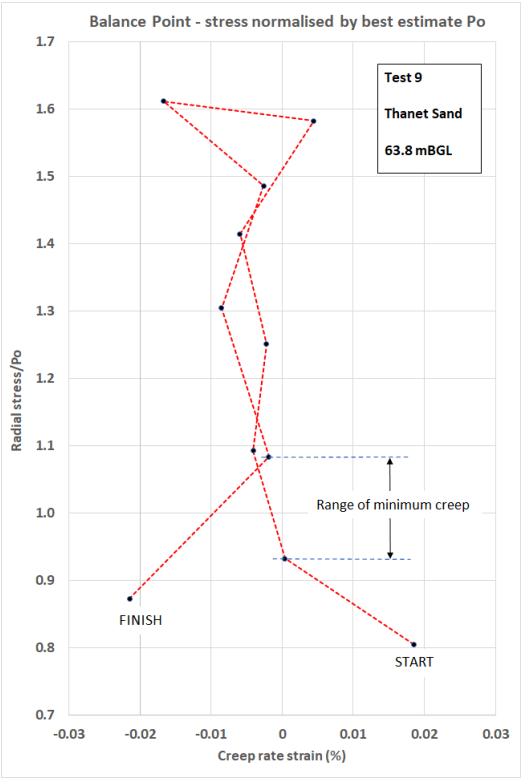

Fig 3.14 BPC analysis

There is an excellent degree of agreement between the best estimate value and the indications from the creep data.

The BPC method can be applied to tests in sand but it is harder to recognise the point where the creep rate is zero. Fig 3.14 is an example of a BPC analysis from a very dense sand. The test was carried out with a small pre-bored pressuremeter.

Procedurally, what is being done with the BPC is similar to the Ménard methodology of applying pressure increments at the start of the test and waiting for a fixed period. The difference is that following pre-boring the borehole has been completely unloaded.

If the material is soil then the consequence is irrecoverable disturbance and very little can be determined until the effects of that have been erased. This requirement is satisfied by a large expansion of the cavity and a subsequent unload that is stopped for the BPC test before the membrane loses contact with the borehole wall.

In fig 3.11, for example, the BPC cycle has a similar stiffness to the unload/reload cycles carried out on the loading. This is not the case for the initial loading of a pre-bored cavity, where the creep due to moving either side of the geostatic stress potentially is overwhelmed by the magnitude of the creep deformation caused by the process of restoring the cavity to its original dimension.

Nevertheless, despite these cautions, it is possible that creep readings on the initial loading are showing a significant response. Fig 3.15 is extracted from the same test as shown in fig 3.14.

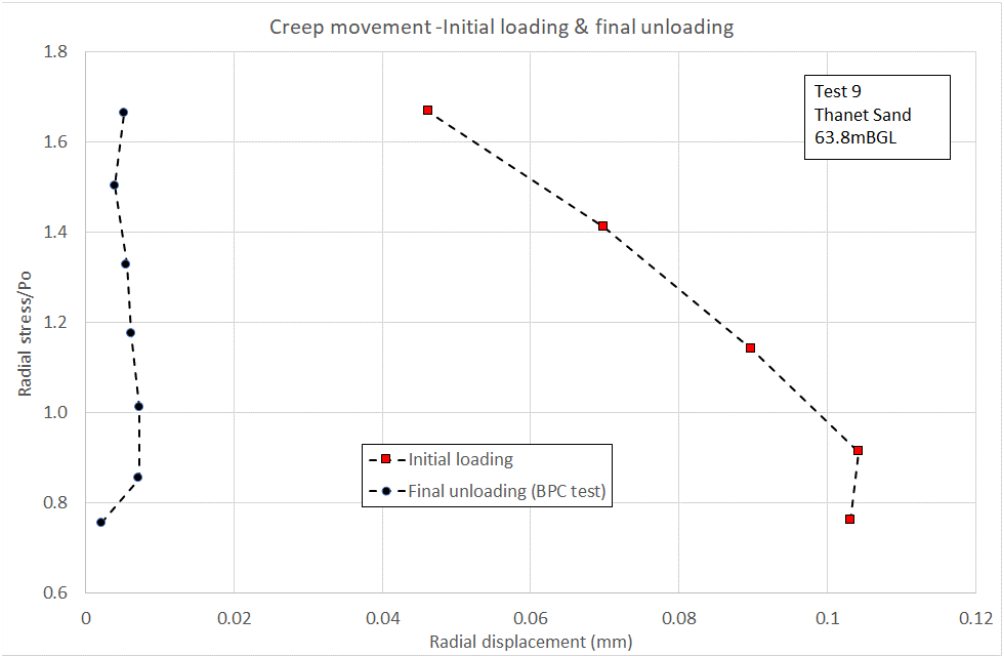

Fig 3.15 Initial loading and final unloading creep compared

The magnitude of the creep is much less for the final unloading. However the initial loading is showing a change of direction in the vicinity of the geostatic stress that would give a zero creep rate. This is not the stress point that would be identified as cavity reference pressure in the standard interpretation of such data.

3.7 A note about k_o – submerged measurements

> *The principle of effective stress is fundamentally important in soil mechanics. It must be treated as the basic axiom, since soil behaviour is governed by it.*
>
> *Changes in water level below ground (water table changes) result in changes in effective stresses below the water table. Changes in water level above ground (e.g. in lakes, rivers, etc.)* ***do not*** *cause changes in effective stresses in the ground below.*
>
> *The coefficient of earth pressure at rest can be defined as that state of stress equilibrium where there are no strains in the lateral direction. If the effective vertical stress is unaffected by changes in the water level above ground level then the same must be true of the effective lateral stress, otherwise the condition of no lateral strain will be violated. Therefore whatever water pressure u is being deducted from the total vertical stress to give effective vertical stress is the same u that must be deducted from the total lateral stress.*
>
> http://environment.uwe.ac.uk/geocal/SoilMech

The statement above is a text-book description of the relationship between effective stress and the coefficient of earth pressure at rest, k_o. The ambient water pressure u_o is deducted

from both the total insitu vertical stress σ_{vo} and the total insitu horizontal stress σ_{ho} to give k_o:

$$k_0 = (\sigma_{ho} - u_0)/(\sigma_{vo} - u_0) \quad [3.6]$$

When applying this to a submerged soil, care has to be taken to establish exactly what it is measured with the pressuremeter to get the appropriate parameters for calculating k_o.

Figure 3.16 Effective stresses, submerged case

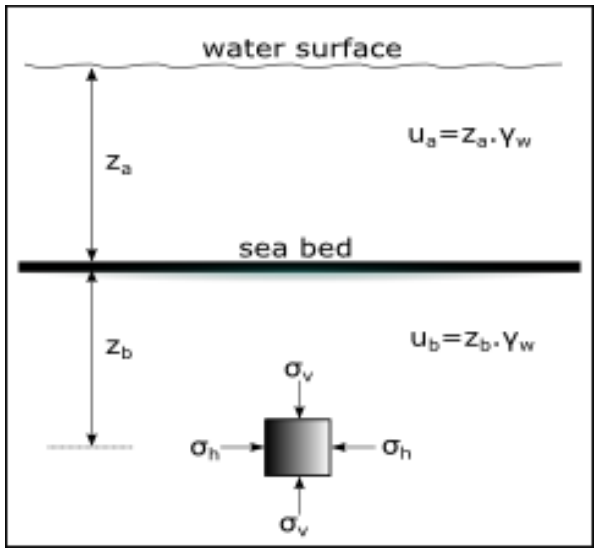

Figure 3.16 is the arrangement for a submerged soil, where u_a is the water pressure above sea bed calculated from the water depth z_a and u_b is the water pressure below sea bed calculated from the soil depth z_b.

The total insitu vertical stress is the weight of everything above the element of soil in fig 3.16:

$$\sigma_{vo} = \gamma_s z_b + u_a \quad [3.7]$$

where γ_s is saturated unit weight of the soil

u_a is the water stress above the sea bed = $z_a\gamma_w$

γ_w is the unit weight of water

The effective insitu vertical stress is σ_{vo} less the contribution of the water:

$$\sigma'_{v0} = \sigma_{vo} - u_a - u_b \quad [3.8]$$

where u_b is the water stress below the sea bed = $z_b\gamma_w$

Because u_a appears in [3.7] and [3.8] it cancels out in the calculation of effective vertical stress:

$$\sigma'_{v0} = \gamma_s z_b - u_b \quad [3.9]$$

Or

$$\sigma'_{v0} = z_b(\gamma_s - \gamma_w) \quad [3.10]$$

Equations [3.9] and [3.10] make no mention of the water above the sea bed and satisfy the condition that the *effective* vertical stress is unaffected by changes in the water level above bed level. However, unlike [3.8], they cannot be re-arranged to find the *total* vertical stress when the material is submerged. A similar argument applies to the *total* insitu horizontal stress, σ_{ho}. The head of water above the soil element is a component of σ_{ho}, and this combination is the stress determined from the pressuremeter test, referred to as cavity

reference pressure p_o. If the process of forming the cavity has not altered the insitu stress state then the following applies:

$$p_0 = \sigma'_{ho} + u_a + u_b \quad [3.11]$$

The effective insitu horizontal stress is the cavity reference pressure less the contribution of the water pressure:

$$\sigma'_{ho} = p_0 - u_a - u_b \quad [3.12]$$

Because the measured parameter is p_o it turns out to be necessary to know u_a, the pressure of the water above the ground surface. k_o is calculated by combining [3.8] and [3.12] giving

$$k_o = \frac{p_o - u_a - u_b}{\sigma_{vo} - u_a - u_b} = \frac{\sigma'_{ho}}{\sigma'_{vo}} \quad [3.13]$$

Note also that when calculating the water contribution (u_a and u_b) the density will not necessarily be that of fresh water. Salt or briny water will have a higher unit weight.